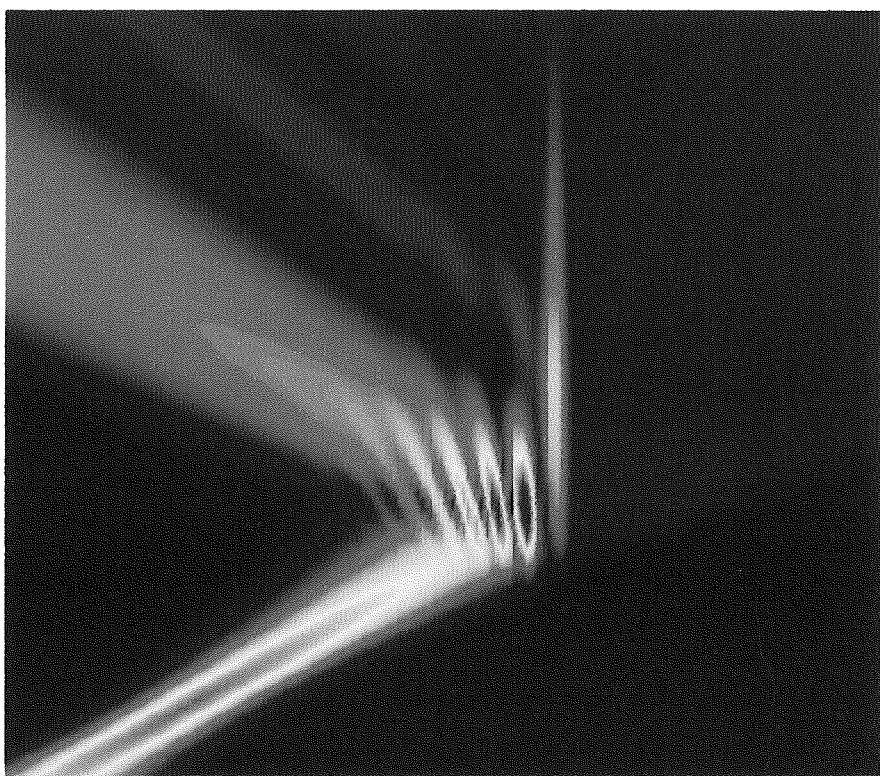


Universitat Autònoma de Barcelona

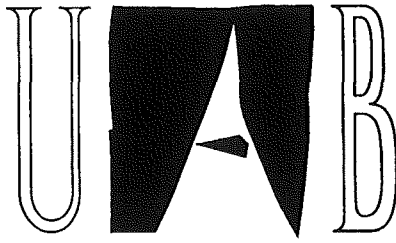
QUANTUM MONTE CARLO SIMULATION OF TUNNELLING DEVICES USING WAVEPACKETS AND BOHM TRAJECTORIES



Xavier Oriols Pladevall



April 1999



Universitat Autònoma de Barcelona

**QUANTUM MONTE CARLO SIMULATION OF
TUNNELLING DEVICES USING
WAVEPACKETS AND BOHM TRAJECTORIES**

Memòria presentada per en
Xavier Oriols i Pladevall per
optar al grau de
Doctor en Enginyeria Electrònica.

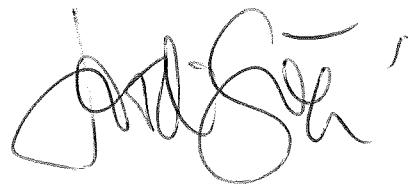
Bellaterra, Abril 1999

En Jordi Suñé Tarruella, professor titular d'Electrònica del Departament d'Enginyeria Electrònica de la Universitat Autònoma de Barcelona,

CERTIFICA

que la memòria QUANTUM MONTE CARLO SIMULATION OF TUNNELING DEVICES WITH WAVEPACKETS AND BOHM TRAJECTORIES que presenta en Xavier Oriols i Pladevall per a optar al grau de Doctor en Enginyeria Electrònica, s'ha realitzat sota la seva direcció.

Bellaterra, Abril 1999



Dr. Jordi Suñé i Tarruella

“I think I can safely say that nobody understands quantum mechanics”

Richard Feynman

[The character of physical law 1965]

Acknowledgements

I have read somewhere that science has to be considered as a type of culture at the same level as painting, playing music or writing poetry. It indicates the human development of the society. However, science is also an economical motor of our society because it has a direct impact on our everyday life. I do not know if the present work will participate in this progress (who knows?), but I can safely say that, like the modest artist that tries to express himself in his own work without worrying about anything else, I have tried to do the best of myself in this work, sincerely and honestly.

First of all, I want to express my most sincere gratitude to Jordi Suñé, my thesis advisor, for lots of things he has done for me during these years at the University. But specially, for making me enjoy our research together and for providing me with the essential techniques to start 'painting' my thesis. I also want to mention Ferran Martín for his constant support during these years and for encouraging me in everyday scientific problems.

I can not forget the *Grupo de Física Aplicada* of *Universidad de Salamanca* that introduced me in the Monte Carlo method using an intuitive picture (one of the fundamental keys of the present work). I really appreciate his extraordinary charming welcome during my stage in Salamanca. Specially, I want to thank Javier Mateos from who I have learned a lot (and not only about the Monte Carlo technique or the *cuisine italienne et francais*).

I also want to express my gratitude to the people from the IEMN (*Institute de Electronique et microelectronique du Nord*) at Lille. Their support during the rainy six months that I spent there, was simply 'magnifique'. The IEMN, is one of these privileged places where you can realise how the scientific knowledge travels from the blackboards to the electronic devices at home. In this regard, I really want to express my sincere gratitude to Didier Lippens and Olivier Vanbesien for their support in my scientific work.

Last, but not least, I want to express my sincere gratitude to all the people of the *Departament d'Enginyeria Electrònica* from *Universitat Autònoma de Barcelona* where this thesis was born and has grown. In particular I want to mention Núria Barniol, Montserrat Nafría, Francesc Pérez and Xavier Aymerich for his fruitful support in my everyday work at University. In the same regard (perhaps in a most informal way), I want to thank Gabriel Abadal, Rosana Rodríguez, Jesús Vizoso, Joan García, Xevi Borrísé, David Jiménez and Arantxa Uranga for his friendship during these years.

I want to mention my family and my friends. I am very grateful to my parents and my sister for a lot of things. I also want to express my most sincere gratitude to all my friends for lots of things that I do not know how to

Acknowledgements

write in this paper, but their definition is contained in the word friends. Several of them are already mention; the rest remains in my mind.

Finally, I also want to express my gratitude to all people that I forget (or I do not dare) to mention who have allowed me to 'paint' this thesis and finish it just before the chaotic beginning of the year 2000.

Xavier Oriols.

Castellsapera,
April 1999.

CONTENTS

Acknowledgements

Contents

List of papers included in this thesis

1. INTRODUCTION.....	11
1.1.- Evolution of semiconductor electronics.....	11
1.2.- Resonant tunnelling diodes.....	12
1.3.- Simulation approaches for resonant tunnelling diodes.....	16
1.3.1.- Landauer-Büttiker approach.....	17
1.3.2.- Density matrix and Wigner Function.....	19
1.3.3.- Non-equilibrium Green's function formalism.....	22
1.4.- Outlines of our approach.....	23
References.....	24
2. CAUSAL TRAJECTORIES IN QUANTUM MECHANICS.....	27
2.1.- The De Broglie-Bohm interpretation of Quantum Mechanics.....	27
2.1.1.- Controversies on the Copenhagen interpretation of quantum mechanics.....	27
2.1.2.- The De Broglie-Bohm's interpretation of quantum mechanics.....	29
2.1.3.- Additional information provided by De Broglie-Bohm approach...34	
2.2.- Properties of Bohm trajectories.....	34
2.2.1.- Bohm trajectories associated to time-independent states.....	35
2.2.2.- Bohm trajectories associated to time-dependent wavepackets.....	38
2.2.3.- Bohm trajectories associated to the density operator.....	41
References.....	45

3. QUANTUM MONTE CARLO SIMULATION.....	47
3.1.- Classical Monte Carlo technique.....	47
3.2.- A quantum Monte Carlo simulator for resonant tunnelling diodes.....	49
3.2.1.- Quantum Monte Carlo in the quantum region.....	51
3.2.2.- Matching classical/quantum trajectories.....	52
3.2.3.- Classical Monte Carlo in the lateral regions.....	53
3.2.4.- Classical Contacts.....	54
3.3.- Simulated results for resonant tunnelling diodes.....	54
3.3.1.- Evaluation of macroscopic results.....	54
3.3.2.- Simulated results.....	56
3.4.- Connection between our approach and the Liouville equation.....	59
3.5.- Possible ways to introduce scattering mechanisms within our.....	61
quantum Monte Carlo simulation	
References.....	63
4.- CONCLUSIONS.....	67

List of symbols

List of acronyms

Papers

LIST OF PAPERS INCLUDED IN THE THESIS

This thesis is based on the following papers, which will be referred by alphabetical letters.

[PAPER A] X.Oriols, J.Suñé, F.Martin and X.Aymerich, *Stationary modelling of 2D states in resonant tunnelling diodes*, J.Appl.Phys, v:78 (3), p:2135, (1995)

This paper is devoted exclusively to propose a new formulation for quasi-bound states. These particular states are important for the correct simulation of resonant tunneling diodes. By a proper choice of the boundary conditions, we showed that these states contain all relevant information of the quasi-2D (system under steady state conditions) including coherence and scattering. This article is briefly explained in section 1.3.1 in the context of the Landauer-Büttiker approach.

[PAPER B] J.Suñé, X.Oriols, F.Martin and X.Aymerich, *Bohm trajectories and their potential use for the Monte Carlo Simulation*, Applied Surface Science v:102, p:255, (1996)

In this paper, we start to study Bohm trajectories associated time dependent wavepacket. Although quite preliminary, it is also the first paper where we point out the possibility of using Bohm trajectories for the simulation of RTD.

[PAPER C] X.Oriols, F.Martin and J.Suñé *Oscillatory Bohm trajectories in Resonant Tunneling structures*, Solid State Communications, v:99 (2), p:123, (1996)

In this work, we show that scattering eigenstates provide unphysical results when dynamic information is required. Hence, Bohm trajectories associated to these states also reproduce these unphysical results. Using time dependent wavepackets, the behaviour of Bohm trajectories is studied showing that they perfectly reproduce our intuitive understanding for tunneling. We can say that this paper is the origin of one of the fundamental points of the present thesis.

[PAPER D] X.Oriols, F.Martin and J.Suñé *Implications of the non-crossing property of Bohm trajectories in one dimensional tunneling configurations*, Physical Review A., v:54(4), p:2595, (1996)

This paper is devoted to study several practical implications of the noncrossing property of Bohm trajectories. Tunnelling times are discussed within the Bohm's interpretation. On the other hand, the intuitive interpretation of the scattering of wavepackets by potential barriers is discussed. In particular, it is shown that claims that Bohm's approach leads to counterintuitive results are subjective.

[PAPER E] J.Suñé, X.Oriols, J.J.Garcia, J.Suñé, T.González, J.Mateos and D. Pardo, *Bohm trajectories for the modeling of tunneling devices*, Microelectronic Engineering, v:36, p:125, (1997)

This paper is the first directly devoted to explain the quantum Monte Carlo method. Although it shows quite preliminary results, it points out the basic directions we have followed. The article contains a study of Bohm trajectories in MOS structures. These work and the last one has been done in collaboration with the group of the University of Salamanca who has provided the classical Monte Carlo algorithm.

[PAPER F] X.Oriols, J.J.Garcia, F.Martín, J.Suñé, T.González, J.Mateos and D.Pardo, *Quantum Monte Carlo Simulation of Tunneling Devices Using Bohm Trajectories*, Phys. Stat. Sol. (b), v:204, p:404, (1997)

Following the path initiated by the previous article, we present self-consistent I-V curve for resonant tunnelling diodes. The origin of this paper was a conference held in Berlin (HCIS'97) where we could realise, for the first time, the opinion of the scientific community about our work.

[PAPER G] X.Oriols, J.J.Garcia, F.Martín, J.Suñé, T.González, J.Mateos and D.Pardo *Bohm trajectories for the Monte Carlo Simulation of quantum-based Devices*, Applied Phys. Letter, v:72, p:806, (1998)

We can say that this paper explicitly shows the technical viability of using Bohm trajectories to extend the classical MC technique to tunnelling devices. Although, quite briefly explained, it contains most of the third chapter of this thesis. As the previous ones, the article has been done in collaboration with the group of the University of Salamanca.

[PAPER H] X.Oriols, J.J.García, F.Martín, J.Suñé, T.González, J.Mateos ,
D.Pardo *Towards the Monte Carlo simulation of resonant
tunnelling diodes with Bohm trajectories and wavepackets*,
Accepted for publication in *Semiconductor Science and
Technology*.

In this paper, our proposed description for quantum Monte Carlo is rewritten in terms of the density matrix. It is shown that, neglecting scattering, the off-diagonal terms of the density matrix remain identically zero even if time-dependent wavepackets are used. Sections 2.2.3, 3.4 and 3.5 of the present thesis are directly related with this paper. Somehow, it can be said that this paper closes our work since it demonstrate the connection between our approach and the ones based on the Liouville equation.

Chapter 1

INTRODUCTION

1.1.- Evolution of semiconductor electronics

During the last 40 years, the understanding of the electronic transport in conventional devices has been based, whenever this was possible, on avoiding the consideration of quantum mechanical (QM) features for electrons, thus promoting a classical intuitive picture. In this regard, after assuming the semiconductor band theory and the Fermi-Dirac statistics, electrons have been pictured as classical particles responding with an effective mass to the external electric field. This simple picture breaks down when the device active dimensions are of the order of the electron's wavelength [Lüth 1995]. Nowadays, the inadequacy of the classical picture for electrons is becoming of actual concern because the commercial Si-CMOS devices are arriving at nanometric dimensions.

Apart from commercial devices, during the 1980s, it started to become possible to fabricate very small prototype devices, whose dimensions are intermediate between the microscopic objects (like atoms) and the macroscopic ones. These are the so-called mesoscopic devices whose characteristic dimensions are of several nanometers. The electronic transport in these mesoscopic devices can only be understood by assuming additional quantum 'skills' features for the electrons such as tunnelling or energy discretization. However, although we can argue that semiconductor devices have been continuously reducing their size since the beginning of solid state electronics 50 years ago, it is difficult and naive to anticipate the actual impact of these mesoscopic devices on electronics industry. In Datta's words

[Datta 1998]: *"The current status of mesoscopic physics thus seems somewhat like that of semiconductor physics in the 1940s, when there was no reason to believe that vacuum tubes would ever be displaced. But...who knows?"*

Anyway, it seems that the study of current flow in small conductors (either commercial or prototype ones) will continue to produce new exciting quantum physics during the coming years, that will either force our classically oriented intuition to assume more and more quantum electron properties, or ,*who knows?*, contribute to a new understanding of QM. In this regard, in the summary of the proceedings of a recent conference we can find the following paragraph written by Ridley [Ridley 1997]:*"... with the possibility of coherent quantum devices in the offing, and the availability of high-speed optical techniques, it is interesting to speculate what a study of non-equilibrium carrier dynamics in semiconductors can contribute to one of the most puzzling features of nature, namely, the collapse of the wavefunction"*.

The objective of the present work is the study of one of these mesoscopic devices which is quite close to reach a commercial status. We concentrate here on the double barrier resonant tunnelling diode (RTD) and, in particular, we develop a Monte Carlo (MC) simulator trying to extent the semiclassical electron picture to this type of mesoscopic device.

1.2.- Resonant tunnelling diodes

One of the attractive features of working with mesoscopic devices is the ability of applying textbook QM to understand their behaviour and still achieving a reasonable degree of success in this task. Perhaps, the most characteristic example is the electron transport by tunnelling (electrons are able to cross energetically forbidden regions, thus violating the most elementary laws of classical mechanics).

Single barrier tunnelling has found widespread applications in both basic and applied research (the latest example is scanning tunnelling microscopy, which allows to 'see' in atomic dimensions [Binning 1982]). It is well known that tunnelling current through a single potential barrier depends exponentially on the height and width of the barrier. Thus, it might seem that the current-voltage characteristic of two barriers in series could not be much more interesting than that of a single barrier. However, if the region between the two barriers is only a few nanometers long (a fraction of the de Broglie electron wavelength), the current-voltage characteristic is qualitatively different from that of a single barrier. In particular it can be easily shown that at certain energies, electrons can traverse the double barrier with near unity transmission probability.

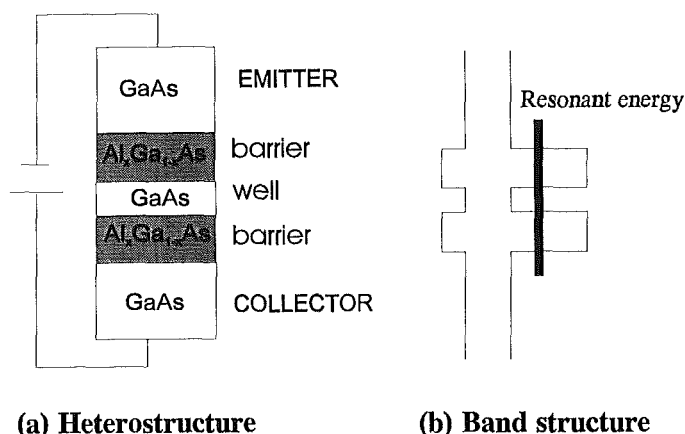


Fig. 1.1: (a) Basic configuration for a typical RTD and (b) Related conduction and valence bands structure.

The basic RTD configuration is a double barrier structure of nanometer dimensions, including two contacts as depicted in figure 1.1. The emitter and collector regions are heavily doped contacts made from a semiconductor with a relatively small bandgap. Between them, two potential barriers are made from a semiconductor with a larger bandgap. The region between the two barriers, called the quantum well, is made again from the smaller bandgap semiconductor. Several different material systems can be chosen if the RTD pseudomorphic growth is assured. Among them, the possibilities offered by the binary, ternary and quaternary III-V semiconductor are multiple and allow the modulation of the values of barrier height and electron effective mass (an example of *band gap engineering*). Moreover, in the literature, we can find RTD with additional layers that provide even more control on several particular aspects of their performance [Burgnies 1997].

The current-voltage characteristic of a RTD is easily understood if we note that the quantum well acts like the typical ‘one dimensional quantum box’: the electron energies associated to perpendicular transport inside the quantum well can only take several discrete values. Let us assume that the quantum well is small enough that, within the energy range of interest, there is only one allowed energy inside the well that we call resonant energy (see figure 1.1b). Then, the structure acts like a filter that only lets electrons with energy near the resonant one to be transmitted. The applied bias, that makes electrons to travel from emitter to collector, modify the whole conduction band geometry lowering the resonant energy as the bias is augmented (see figure 1.2). Thus, the current increases as the resonant energy approaches the most populated energy electrons in the collector. But, when the resonant energy falls below the conduction band edge in the emitter, there is almost any electron that can traverse the barrier, thus forcing the current to decrease to its valley value. Finally, at high bias, electrons pass over the barrier leading to another increase of the current. This is the qualitative explanation

of the origin of the negative resistance in the RTD. The figures of merit for this device are the peak current and the rate between the peak to the valley current. The improvement of both magnitudes in real devices is quite difficult since they generally respond inversely to any RTD modification (such as barrier dimensions, doping concentrations, ...) [Vanbesien 1991].

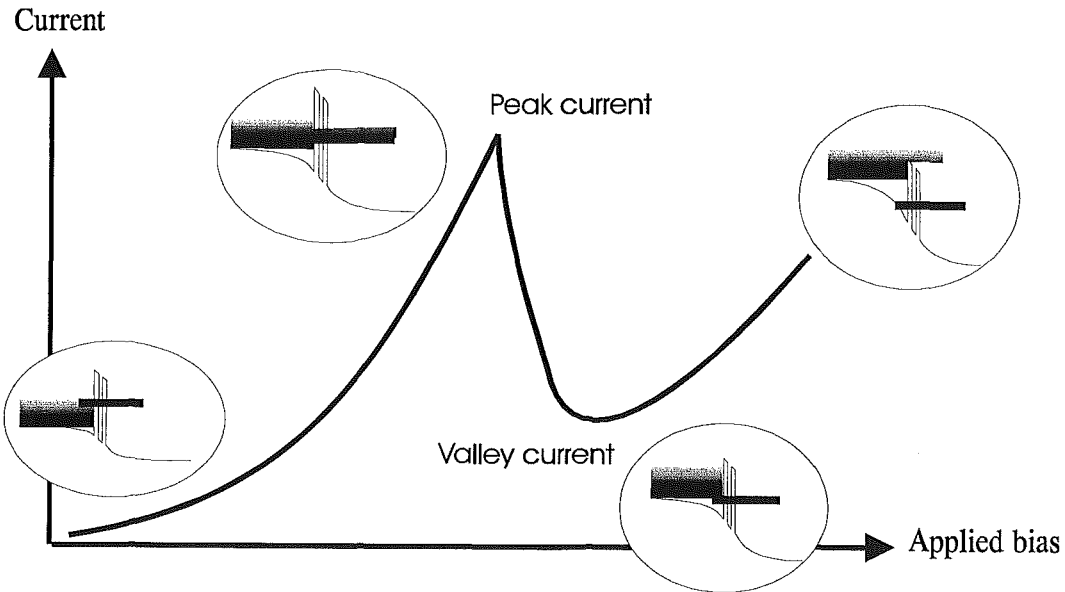


Fig. 1.2: schematic representation of the I-V curve of a typical RTD. The resonant energy inside the QW acts like an energetic filter that lets the electrons from the emitter to arrive at the collector.

In the 50s, Bohm already solved this problem (the academic double barrier potential) in one of his quantum theory textbooks [Bohm 1951]. After recognising that this phenomenon could be projected with electrons in order to provide new electronic device, Tsu and Esaki [Tsu 1973] showed that negative resistance could arise from finite superlattices. A year later, together with Chang [Esaki 1974], they were the first to observe resonant tunnelling oscillations in a semiconductor. Ten years later, Sollner *et al.* [Sollner 1983] showed that the intrinsic charge transport inside the double barrier could respond to voltage changes in times of the order of 0.1 ps, thus opening the path for RTD high frequency applications. It is argued that the negative resistance and this fast intrinsic time response offer quite interesting applications in analogic electronics for frequency generation, detection or multiplication in the millimetric and submillimetric regim. Brown *et al.* [Brown 1991] have observed RTD oscillations at 712 GHz, which are the highest frequency ever achieved with a solid-state source. On the other hand, in digital electronics, several efforts are devoted to integrate RTD in CMOS logic circuits with the double goal of reducing complexity and augmenting the operation frequency [Mazumder 1998]. Finally, regarding power

capability (one of the practical problems that limits its introduction in commercial circuits), power densities of 1 kW/cm^2 have already been obtained within GaAs/AlAs [Bouregba 1993].

As an example, in figure 1.3, we show several typical experimental I-V curves obtained at the *Institute d'Electronique et Microelectronique du Nord* (IEMN), in 1998, which can be considered as an example of the *state-of-the-art* RTDs. Finally, let us say that, to our knowledge, in spite of these unquestionable potential applications, there is still no commercial RTD-based device on the market although it is argued that RTD are quite near to reach a commercial status (see for example [Seabaugh 1998]).

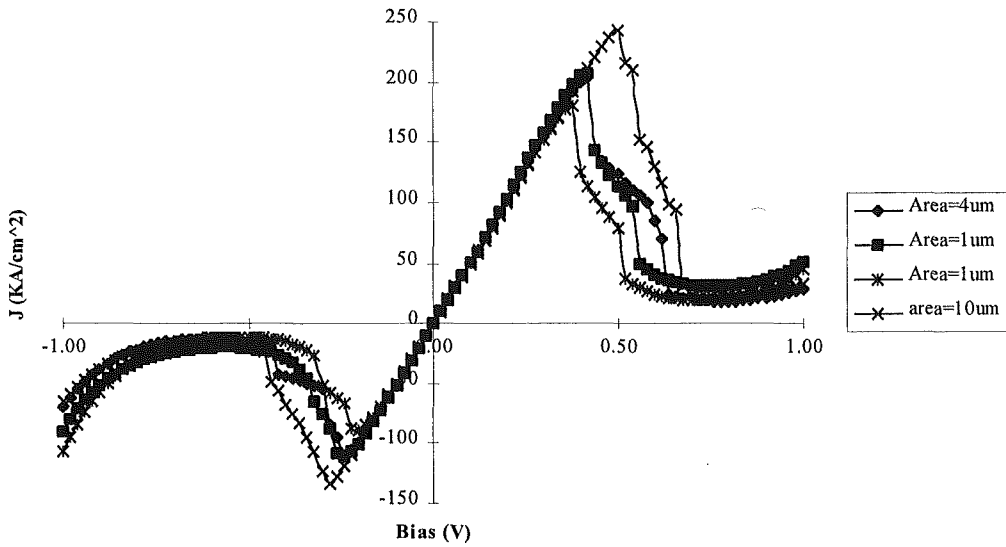


Fig. 1.3: Experimental I-V curves for a $\text{In}_{0.53}\text{Ga}_{0.47}\text{As}/\text{AlAs}$ RTD of 17 \AA barrier and 45 \AA well for several device Areas.

On the other hand, more than a thousand scientific papers about RTD have been published in the scientific literature. This shows the enormous interest that RTD has attracted in the research community. Such structures represent a suitable opportunity for the theorists to understand electronic transport in mesoscopic devices. As we have pointed out, one has to consider the quantum coherence of electrons to allow them to pass through thin barriers, but several scattering mechanisms can break the electron phase coherence and destroy the coherent picture explained in figure 1.2. Additionally, to obtain realistic simulations, the charge density at any point has to be computed with a Poisson solver to find self-consistent potential profiles. And finally, there are two contacts (reservoirs) that connect the RTD with the

exterior, so RTDs have to be treated as an open system. Let us summarised the complexity of the RTD simulation in Capasso's words [Capasso 1990]: "*this (RTD simulation) implies the need of a fully quantum mechanical and self-consistent calculations in the presence of scattering and coupling to the reservoirs(contacts), a formidable task indeed!*"

1.3.-Simulation approaches for resonant tunnelling diodes

In conventional devices, it is assumed that an electron is perfectly defined by its position x and momentum $p=\hbar\cdot k$, and that the evolution of both magnitudes, between scattering events, is described by classical mechanics. In this regard, the fundamental quantity for the simulation of conventional devices is the carrier distribution function, $f(x,k,t)$, which specifies, at any time t , the number of carriers located at the position x that have a momentum p . This distribution is a solution of the Boltzmann transport equation (BTE) that simultaneously deals with Newton dynamics and scattering processes.

However, as we have shown in the previous section, the classical picture for electrons is not adequate to understand RTDs. Moreover, the RTD system is very different from a simple isolated quantum system, where a conservative Hamiltonian can be readily formulated with the appropriate boundary conditions. Instead of this, the complete simulation of a RTD has to take into account a full quantum system with both particle and energy exchanges with the device's environment. On the other hand, the tunnelling current depends exponentially on several parameters, such us barrier dimensions, which are not perfectly determined in real devices. These two factors explain why, in spite of the several tools developed during the last 30's years, it is still a *formidable task* to accurately predict the I-V characteristic of RTDs.

In the present section, we will briefly discuss some representative approaches found in the literature for the modelling and simulation of RTD. Common to all quantum transport approaches, one takes a model function to represent electrons in the quantum system. Once the model function is evaluated for a specific device, under particular boundary conditions, other physical quantities of interest can be calculated from it. It is the chosen model function that makes major differences (in terms of the mathematical complexity, capabilities and results) between the different approaches. Mainly, existing RTD device models can be classified as either coherent or kinetic. In the coherent models, the model function is typically the wavefunction solution of the Schrödinger equation (rigorously speaking: the envelope function), while in kinetic models, the density matrix, the Wigner function or the Green's functions are employed. The big difference between coherent and kinetic models is that coherent transport is based on single-particle (i.e. pure state), while kinetic models are based on many particle descriptions (i.e. mixed states). Hereafter, we will present three of these

models: the Landauer-Büttiker approach (the most symbolic kind of coherent models), and the density matrix and the Green's function as two types of kinetic models.

1.3.1.- Landauer-Büttiker approach

The Landauer-Büttiker approach has been widely used in the interpretation of mesoscopic devices with a reasonable success. It is supposed that the current through a conductor is only expressed in terms of the transmission probability of electrons injected from the external contacts. In this regard, each electron inside the device is assumed to be described by a wavefunction $\varphi_n(x)$ solution of the time-independent Schrödinger equation (i.e. the model function in this coherent approach is the wavefunction). The current density of the state in each position is computed applying the standard current operator, and the charge density is proportional to the modulus of the wavefunction. On the other hand, a distribution function $f(k)$ (position independent) is associated to each state. States associated to electrons departing from the emitter are supposed to be occupied by the emitter contact distribution and, obviously, states associated to electrons incidents from the collector, are occupied according to the collector contact distribution (see fig 1.4). The total current (or the charge) is computed as a sum over the current (charge) of each state weighted by the distribution function $f(k)$.

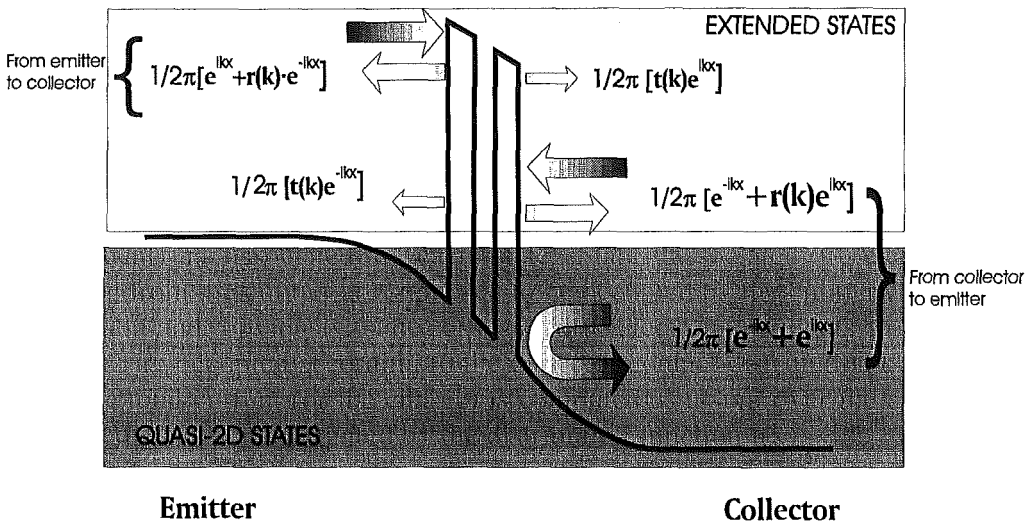


Fig. 1.4: Mathematical description of the different states involved in the calculations of the net current within the Landauer-Büttiker approach.

Let us notice that the consideration of the RTD as an open system implicitly sets the Schrödinger boundary conditions for each eigenstate $\varphi_n(x)$. There are, basically, two kinds of states: (i) the extended states which are associated to electrons incidents from one contact and that are partially transmitted and

reflected through the device (see the clearer square in figure 1.4), and (ii) the one side-bound states which are associated to electrons bounded in the emitter region and therefore totally reflected by the potential profile (see darker square in figure 1.4). In 1989, Krivan *et al.* demonstrated that these states form an orthogonal and complete base of the RTD quantum system (with no collision term in the Hamiltonian) [Krivan 1989]. Although their demonstration was quite controversial, Di Carlo *et al.* confirmed their result with a different approach [Di Carlo 1994].

Limitations of the Landauer-Büttiker approach: quasi-2D states

As we have said, the often described Landauer-Büttiker approach has been proved to be very useful in describing mesoscopic transport since it is intuitively very appealing to assume that the conductance of a sample is proportional to the ease with which electrons can transmit through it. However, one can wonder if this approach is accurate enough. *Does the scattering mechanisms affect the conductance in real mesoscopic devices?* It is argued that if the electron transport is coherent (i.e. the distances involved are shorter than the electron mean free path and phase-relaxation length) then the Landauer-Büttiker approach is rigorously correct. Unfortunately, the electron transport in real RTD can not always be considered as coherent.

In order to clarify the limitations of this approach (i.e. the meaning of coherent transport), let us concentrate on one kind of one-side bound state that we will call quasi-2D states. We define them as states incident from the collector but with an important presence probability in the barrier. In a fully coherent quantum picture, these states do not contribute to the net total current, but only to the charge. However, from a physical point of view, the electrons located in the emitter quantum well and associated to quasi-2D states, can contribute to the net current in a two step process: (i) electrons incident from the emitter can reach these states by a dissipative collision (non coherent transport) and, then (ii) these electrons can contribute to the total net current by traversing the barriers by tunnelling. However, the Landauer-Büttiker approach can not model this physical phenomenon since quasi-2D states are totally reflected states (i.e. they do not carry any current). In [paper A] we propose a new definition for the quasi-2D states that can overcome these limitations.

The conventional boundary conditions for quasi 2-D states impose that the modulus at the emitter is zero $|\varphi_n(x \rightarrow -\infty)|^2 \rightarrow 0$. This implicitly implies that the wavefunction is real and, hence, that this state does not contribute to the current. However, we propose a new physical boundary conditions for these states to be able to describe their stationary contribution to the charge and current densities: (i) Since in the collector region we want the current to be uniform, the most obvious choice is a transmitted plane at this region, and (ii) since they are bounded at the emitter we also propose $|\varphi_n(x \rightarrow -\infty)|^2 \rightarrow 0$.

These two boundary conditions are not simultaneously compatible for an eigenstate of the Hamiltonian. However, these two conditions can be satisfied by two different real eigenstates, $\varphi_{n1}(x)$ and $\varphi_{n2}(x)$ (for two slightly different values of the energy, E_{n1} and E_{n2}). We propose to describe the quasi-2D state by the combination of the two eigenstates:

$$\varphi_n(x) = \varphi_{n1}(x) + j\varphi_{n2}(x) \quad (1.1)$$

Within our model, the charge is computed from the wave-function moduli and the current applying the current standard operator. Moreover, with a proper choice of their occupation function, we have found that they perfectly model the previously presented steady-state situation without explicitly considering inelastic interaction. For a complete description of the present model see [paper A].

1.3.2.- The Density matrix and the Wigner Function

As we have previously argued (and explicitly pointed out for quasi-2D states), the description of the quantum system by a complete set of eigenstates does not always provide an accurate simulation for RTDs (In informal words, once scattering is introduced, it is, in general, difficult to associate a single wavefunction to each electron). However, there are other approaches developed with the goal of introducing scattering in the RTD. Among them, the density matrix, $\rho(x, x', t)$ (or its Wigner-Weil transformation: the Wigner distribution function, $f_w(x, k, t)$), is a very useful tool that facilitates the simultaneous applications of the postulates of the quantum mechanics and the results of the statistical calculations.

From a mathematical point of view, the density matrix is the solution of the Liouville equation that, in the x -representation, can be written as:

$$\frac{\partial}{\partial t} \rho(x, x', t) = \frac{i\hbar}{2m^*} \left[\frac{\partial}{\partial x^2} - \frac{\partial}{\partial x'^2} \right] \cdot \rho(x, x', t) - \frac{i}{\hbar} [V(x) - V(x')] \cdot \rho(x, x', t) \quad (1.2)$$

If our device is perfectly described by a single state solution of the Schrödinger equation $\Psi(x, t)$, then the density matrix and the Schrödinger formalism are equivalent approaches. However, the density matrix formalism can deal with other quantum systems that can not be directly studied with the Schrödinger equation. For example, let us suppose a quantum system where we are not able to associate a single state $\Psi(x, t)$ to it, because we only know the probabilities, $\{f_n\}$, of finding the electrons in one of the states $\{\Psi_n(x, t)\}$. Then, the density matrix formalism using this 'incomplete' information, can provide macroscopic results as the charge or the current inside the device [Fano 1957]. Let us develop the density matrix for this particular case. We

suppose that each wavefunction is expanded in a set of eigenfunctions $\varphi_k(x)$ (i.e as a superposition of eigenfunctions) as follow:

$$\Psi_n(x,t) = \int_{-\infty}^{\infty} a^n(k) \cdot e^{i\frac{E_k t}{\hbar}} \cdot \varphi_k(x) \cdot dk \quad (1.3)$$

where $a^n(k)$ is the k -components of the wavefunction associated with the eigenstate $\varphi_k(x)$ whose energy is E_k . Then, the density matrix, in the k -representation, can be written as:

$$\rho(k,k',t) = \sum_n f_n \cdot a^n(k) \cdot a^{n*}(k') \cdot e^{i\frac{(E_k - E_{k'})t}{\hbar}} \quad (1.4)$$

In this representation, k and k' (i.e. the row and the column of ρ) label the set of considered $\{\varphi_k(x)\}$. From equation (1.4) we can provide a more complete definition for coherent and kinetic models. Let us notice that within the Landauer-Büttiker approach, where we assumed that the electrons are described by eigenfunctions $\varphi_{kn}(x)$, the density matrix, in the k -representation, remains diagonal (i.e. $a^n(k) = \delta(k - k_n)$ for Hamiltonian eigenstates). Models with this property are called coherent modes. On the other hand, models where the off-diagonal elements of $\rho(k,k',t)$ are non-zero are called kinetic models (Naively, one can appreciate the importance of the off-diagonal terms by noticing that one must rely on the interference among many plane waves in order to describe the propagation of a single localised wavepacket).

In general, the majority of RTD simulations within this approach do not use directly the density matrix, but a transformed version called the Wigner function, $f_w(x,p)$. The Wigner-Weil transformation operates over the density matrix to provide a more intuitive framework [Hillery 1984]. To obtain it from the density matrix, we first transform the two position variables to the center of mass, x , and relative coordinate, q , and then, we Fourier transform the relative coordinate q to obtain the Wigner function that depends on the position x and momentum p :

$$f_w(x,p) = \frac{1}{(2\pi\hbar)} \int_{-\infty}^{+\infty} dq \cdot e^{i\frac{qp}{\hbar}} \rho(x - \frac{q}{2}, x + \frac{q}{2}) \quad (1.5)$$

Identically, the Liouville equation (1.2) can be Wigner-Weil transformed to obtain a kinetic equation in a pseudo-phase space:

$$\frac{\partial f_w(x,k,t)}{\partial t} = L \cdot f_w(x,k,t) \quad (1.6)$$

where L is the Liouville operator (related with the right term of the equation 1.2) that describes ballistic electron motion (i.e. the behaviour of the Wigner function in the absence of scattering). The formal similarity between the obtained kinetic equation and the Boltzmann equation is rather attractive and several authors have used a collision term, C_{ol} , to take into account the scattering in the RTD simulation. The resulting equation takes the form:

$$\frac{\partial f_w(x, k, t)}{\partial t} = L \cdot f_w(x, k, t) + C_{ol} \cdot f_w(x, k, t) \quad (1.7)$$

The Wigner function is not only useful as a calculation tool but, it is said that it can also provide insights into the connections between classical and Quantum mechanics. However, there is an important difference between the Wigner function, $f_w(x, p)$, and the semiclassical distribution function $f(x, p)$. The Wigner function can not be interpreted as the number of particles that occupy a position x and have a momentum p in the same way as a classical distribution function, because $f_w(x, p)$ it is not always positive. From a practical point of view, Frensley provided appropriate boundary conditions for the simulation of open systems in the Wigner framework [Frensley 1990]. Since then, a lot of profitable work has been dedicated to the simulation of RTD within this formalism. However, quantitative simulations of RTD are still not evident.

At this point, it is convenient to notice the analogies between the semiclassical transport model and the one based on the quantum Liouville equation. The Newton equation, which describes the classical dynamics of electrons, is conceptually replaced by the Schrödinger equation. Identically, the Boltzmann equation, which takes into account the dissipative processes inside the device, is replaced by the Liouville equation.

Other approaches with the Liouville equation

From a practical point of view, in the literature, we can find several attempts to solve the Liouville equation by quite different methods (some of them even quite close to the Landauer-Büttiker model).

Among them, the group of Carlo Jacoboni in Modena works with the Wigner distribution function in order to provide a formalism of electronic transport in terms of Wigner Paths [Brunetti 1997] [Brunetti 1989] [Rossi 1992]. In somehow, although their models have not always a transparent interpretation, one can say that they try to solve the Liouville equation using quite classical concepts. In the same regard, but more recently, Rossi *et al.* [Rossi 1998] have developed a density matrix formulation to study the single wavepacket evolution with scattering inside its dynamic evolution.

On the other hand, the work of Fischetti [Fischetti 1998] is of particular importance for us. He started very interesting discussions about topics that are quite recurrent in this thesis. He argues that it is not always necessary or even desirable to face fully off-diagonal formulations of the Liouville equation to treat the electron transport in mesoscopic devices. Under some conditions of practical interest (sub-50 nm devices), the off-diagonal terms of the density matrix may be neglected. In this regard, he presents a discussion about the actual size of the electron (i.e. its spatial dispersion) which will be repeatedly referenced. Let us provide a simple explanation of his proposal: still assuming that each electron is described by a Hamiltonian eigenstate (extended over the whole device), he introduces the scattering effects via a Pauli master equation discussing its validity as a particular case of Liouville equation. From a practical point of view, although his method provides an accurate intuitive simulation framework for mesoscopic devices, the results for RTD are, for the moment, not very successful.

1.3.3.- Non-equilibrium Green's function formalism

The nonequilibrium Green's functions (NEGF) formalism provides a different mathematical scenario to formally study interactions in QM systems. Electron-electron interactions in the contact regions, electron-phonon interactions, and other scattering processes, can be readily incorporated in a unified and consistent formulation.

The NEGF's model consist of a number of different Green's functions and their related self-energy functions that take into account the scattering mechanism with the desired degree of approximation. Each of these functions, in steady-state problems, can be Fourier transformed to yield an energy-resolved function which is able to take into account the phase-correlation information of the system (i.e. like the off diagonal elements of the density matrix). The central equation for the NEGF approach is the Dyson's equation. Starting from this equation in the Keldysh formalism, Datta, Lake and co-workers formulated a set of equations for RTD steady state transport calculations, which yields dc I-V characteristics [Lake 1997]. Once again, this set of equations combines the Schrödinger equation with a probabilistic description of random scattering processes.

Recent efforts at Texas Instruments, in collaboration with others researches, have produced nanoelectronic modelling (NEMO) software utilizing nonequilibrium Green's functions to attempt state-of-the-art device modelling tool for nanoelectronics devices [Klimeck 1995]. The relevant publications have indicated that the NEMO program may be an accurate modeling for RTD I-V characteristics and other steady-state properties. On the other hand, the development of the NEGF based time-dependent modelling is still in his infancy. See [Datta 1998] to provide further information on the use of Green's functions for mesoscopic devices.

1.4.- Outlines of our proposal

At this point, we want to anticipate the main features of our work. But, before this, let us wonder about the current status of the simulation tools for RTD. Among the different alternatives found in the literature, no one has clearly emerged as the best choice for the simulation of mesoscopic devices. In our opinion, a successful approach requires correctness, but also simplicity. The word simplicity has to be understood twofold. First, from a mathematical point of view, it means to try to find the simplest algorithm that correctly describes the problem. Second, from a physical point of view, simplicity means to be able to provide an intuitive (i.e. an easily understandable) description of the system. However, when quantum transport is involved, simplicity (in both meanings) is not readily achievable. In particular, none of the above mentioned approaches provides neither a simple algorithm nor an intuitive understanding of the quantum devices. This is the main reason, in our opinion, that explains why RTD technology has evolved much faster than the simulation tools. Due to the lack of simplicity of the simulation models, experimentalists have only made extensive use of the Landauer-Büttiker formalism when they have required simulated results.

The full QM kinetic formulations depart from very fundamental equations (Liouville or Dyson equations) using several approximations, each at a time, to be able to develop a numerically tractable tool. For example, let us center on the Wigner formalism. Although, the Wigner function is a formal solution of the Liouville equation, the scattering is generally introduced using the relaxation time approximation [Garcia 1996], that is a quite fuzzy way to treat collisions in quantum systems. Nonetheless, others more rigorous approaches [Brunetti 1997] are numerically non-viable for device simulation proposals. In this regard, these approaches are based on a TOP-DOWN methodology. This usually provides function models which are hard to be numerically manipulated and with a not-always clear physical interpretation (in our example, the negative values of the Wigner function). On the other hand, we are interested in providing a simulation tool starting from a different point of view. We want to simulate mesoscopic devices with a simple (i.e. fully understandable) function model. It is our opinion that such a tool will enhance our understanding of RTD and, perhaps more important, will be able to connect experimental and theoretical work on RTD.

This idea has been partially investigated by other authors. Among them, Salvino and Buot pointed out one direction for a simple and intuitive mesoscopic simulation tool [Salvino 1992]. They proposed to study RTD by extending the classical MC technique to these devices. They defined a device region, called Quantum Window (QW), where quantum phenomena must be considered. Outside this region, they used a classical MC simulator to solve

the BTE. Inside the QW, they considered ad-hoc quantum trajectories to compute all macroscopic results following the MC philosophy. Following their steps, we will develop a quantum MC simulator for RTD based on Bohm trajectories. As we will explain in the second chapter, Bohm trajectories are physical entities that are able to perfectly reproduce Schrödinger-equation results within a classical intuitive framework. In this regard, by using Bohm trajectories, our approach will have the simplicity (from a physical point of view) guaranteed. In this report, we will also present the connections of our work with the ones based on Liouville equation in a BOTTOW-UP development (section 3.4). In other words, although our proposal is based on simple physical ideas we are able to relate it with the density matrix formalism within a mathematical framework. Our proposal, although here focused on RTD because these devices are of high practical interest and show a rich phenomenology, can be readily extended to any mesoscopic device based on QM interference phenomena.

References

- [Binning 1982] G.Binning and H.Rohrer *Scanning tunnelling microscopy* Helvetica Physica Acta v:55, p:726
- [Bohm 1951] D.Bohm *Quantum theory* Prentice-Hall, Engelwood Cliffs, N.J.
- [Bouregba 1993] R.Bouregba, O.Vanbesien, P.Mounix, D.Lippens, L.Palmateer, J.C.Pernot, G.Beaudin, P.Encrenaz, E.Bockenhoff, J.Nagle, P.Bois, F.Chevoir, and B.Winter *Resonant tunneling diodes as sources for millimeter and submillimeter wavelengths*, IEEE trans. on microwave theory and technique, v:41(11), p:2025
- [Brown 1991] E.R.Brown, J.R.Södeström, C.D. Parker, L.J.Mahoney, K.M.Molvar, and T.C.Mcgill, *Oscillations up to 712 GHz in InAs/AlSb resonant tunneling diodes*, Appl. Phys. Lett. v:58(20), p:2291
- [Brunetti 1997] R.Brunetti and C.Jacoboni, *Wave-packet analysis of electron-phonon interaction in the Wigner formalism*, Phys. Rev. B, v:56(23), p:56
- [Burgnies 1997] L.Burgnies *Mecanismes des conduction en Regime balistique dans les dispositifs electroniques quantiques* Thesis presented at l'Université des Sciences et Techniques de Lille
- [Capasso 1990] F.Capasso *Physics of Quantum Electron Devices*, Springer-Verlag

- [Datta 1997] S.Datta, *Electronic transport in mesoscopic systems* Cambridge University Press
- [Di Carlo 1994] Aldo Di Carlo, P.Vogl and W.Pötz *Theory of Zener tunneling and Wannier-Stark states in semiconductors* Phys. Rev. B, v:50(12), p:8358
- [Esaki 1974] L.Esaki and L.L.Chang, *New transport phenomenon in a semiconductor superlattice*, Phys. Rev. Lett., v:33(3), p:495
- [Fano 1957] U.Fano, *Description of States in Quantum Mechanics by the Density Matrix and Operator Techniques*, Reviews of Modern Physics, v:29(1), p:74
- [Fischetti 1997] M.V.Fischetti, *Theory of electron transport in small semiconductor devices using the Pauli master equation*, J. Appl. Phys., v:83(1), p:270
- [Frensley 1990] W.R.Frensley *Boundary conditions for open quantum systems driven far from equilibrium*, Reviews of Modern Physics, v:62(3), p:745
- [Garcia 1996] J.J.Garcia, X.Oriols, F.Martín and J.Sufié, *Comparasion between the relaxation time approximation and the Boltzmann collision operator for the simulation of dissipative electron transport in resonant tunneling diodes* Solid State Elect., v:39(12), p:1795
- [Hillery 1984] M.Hillery, R.F.Cornell, M.O.Scully and E.P.Wigner, *Distribution Functions in Physics Fundamentals* Physics Reports, v:106 (3), p:121
- [Klimeck1995] G.Klimeck, R.Lake, R.Chris Bowen, W.R.Frensley and T.S.Moise, *Quantum device simulation with a generalized tunneling formula*, Appl. Phys. Lett., 67(17), p:2539
- [Kriman 1989] A.M.Kriman, N.C.Kluksdahl and D.K.Ferry, *Scattering states and distribution functions for microstructures*, Phys. Rev. B, v:36(11), p:5953
- [Lake 1997] R.Lake, G.Klimeck, R.Chris Bowen, Dejan Jovanovic, *Single and multiband modeling of quantum electron transport through layered semiconductor devices*, J. Appl. Phys. v:81(12), p:7845
- [Lüth 1995] H.Lüth *Nanostructures and Semiconductor Electronics*, Phys. status Solidi (b) v:192, p:287
- [Mazumder 1998] P.Mazumder, S.Kulkarni, M.Bhattacharya, J.P.Sun and G.Haddad, *Digital Circuits Applications of Resonant Tunneling Devices*, Proc. of the IEEE, v:86 (4) p:662

- [Ridley 1997] Summary of the proceedings of the *Nonequilibrium Carrier Dynamics in Semiconductors*, Physica Status Solidi (b), v: 204, n:1, pag: 1-584
- [Rossi 1992] F.Rossi, P. Poli and C.Jacoboni, *Weighed Monte Carlo approach to electron transport in semiconductors*, Semicond. Sci. Technol., v:7, p:1017
- [Rossi 1998] F.Rossi, A. Di Carlo and Paolo Lugli, *Microscopic Theory of Quantum-Transport Phenomena in Mesoscopic Systems: A Monte Carlo Approach*, Phys. Rev. Lett., v:80 (15), p:3348
- [Salvino 1992] R.E.Salvino and F.A.Buot, *Self-consistent Monte Carlo particle transport with model quantum tunnelling dynamics: Applications to the intrinsic bistability of a symmetric double-barrier structure*, J. of Appl. Phys., v:72, p:5975
- [Seabaugh 1998] A.Seabaugh, X.Deng, T.Blake, B.Brar, T.Broekaert, R.Lake, F.Morris and G.Fraizier, *Transistors and tunnel diodes for analog/mixed-signal circuits and embedded memory* Proc. of the IEDM 1998.
- [Sollner 1983] T.C.L.G.Sollner, W.D.Goodhue, P.E.Tannewald, C.D.Parker, D.D.Peck, *Resonant tunneling through quantum wells at frequencies up to 2.5 THz*, Appl. Phys. Lett., v:43(6) p:588
- [Sun 1998] J.P.Sun, G.I.Haddad, P.Mazumder and J.N. Schulman, *Resonant Tunneling Diodes: Models and Properties* Proc. of the IEEE, v:86, p:641
- [Tsu 1973] R.Tsu, L.Esaki, *Tunneling in a finite superlattice*, Appl. Phys. Lett., v:22 p:562
- [Vanbesien 1991] O.Vanbesien *Simulation et caracterisation electronique des diodes double barrier a effet tunnel resonnant*, Thesis presented at l'Université des Sciencies et Techniques de Lille.

Chapter 2

CAUSAL TRAJECTORIES IN QUANTUM MECHANICS

2.1 The De Broglie-Bohm interpretation of Quantum Mechanics

As we have pointed out, we are interested in describing quantum phenomena inside RTD in terms of single particle trajectories. Among other possibilities, Bohm trajectories fit with our goal because they perfectly reproduce the charge and current densities inside the device. The general philosophical implications about the physical reality of Bohm trajectories are far from the scope of this thesis, however, to be fair, it is quite difficult to present a mathematical description of the de Broglie-Bohm (BB) approach without being seduced to assume its physical interpretation. In this regard, in the present chapter, we present the BB interpretation of QM from a complete (mathematical and physical) point of view.

2.1.1.- Controversies on the Copenhagen interpretation of quantum mechanics

Although the debate about the true nature of the quantum behaviour of atomic systems has never ceased, there are two periods during which it has been particularly intense: the years that saw the funding of QM and, increasingly, these modern times [Selleri 1990]. The dramatic disagreement between scientists is centred around some of the most fundamental questions in science: *Do atomic objects exist independently of human observations and, if so, is it possible for man to understand correctly their behaviour?* Nowadays, the orthodox interpretation of QM (called Copenhagen

interpretation of QM in order to acknowledge the city where it was born) gives a more or less openly pessimistic answer to both questions.

Let us briefly discuss the Copenhagen's negative answer. The first postulates of the robust mathematical apparatus that supports Copenhagen school, affirms that a physical system is *completely* defined by specifying a ket in the state space (a wavefunction in position coordinates). On the other hand, Schrödinger equation incorporates the Heisenberg uncertainty relations since no wavefunction exists that assigns single well-defined values to the position and momentum simultaneously. In this regard, no position and momentum measurement can be done simultaneously in a physical system (and as the system is completely described by the wavefunction), therefore, one concludes that these two observables can not be real at the same time. In formal words, it is not possible to give a causal description of the physical system in space time.

On the other hand, several scientists have stressed the philosophical difficulties in blindly accepting the Copenhagen interpretation of QMs. Among them, for example, Einstein was unable to assume the revolutionary changes in the world view required by the Copenhagen theory. What bothered him most was the elimination of determinism from fundamental physics: "*God does not play dice*". In addition, the Einstein-Podolsky-Rosen paradox, that appeared in the journal *Physical Review* in 1935 [Einstein 1935], used their famous 'criterion of physical reality' to try to demonstrate that the Copenhagen interpretation of QM was not a complete theory. The Bohr's answer [Bohr 1935] to this paradox, that was received by the editor of the same journal less than four months after the previous one, clearly manifested the essence of the disagreement: "*The previous criterion does not exhaust all possible ways to recognise a physical reality*". For Einstein, physics was only a refinement of common sense that aspires to describe reality in space and time. However, Bohr exposed a less ambitious definition of physics as a discipline whose task is not to discover the way nature is, but only to impose order on our experimental measures.

Once more, these discrepancies can be found didactically explained in the Feynmann's lectures on Physics [Feynmann 1963]. Both, Einstein's and Bohr's, physical reality conceptions can be easily understood by noting the two possible answers to the following question: "*If a tree falls in a forest and is nobody there to hear it, does it make noise?*". From a classical point of view, the answer is clear. A real tree falling in a real forest makes a sound, even if nobody is there. However, the standard QM are developed under the idea that we should not speak about those things that we cannot measure. In this regard, Born will affirm: "*I do not need to answer such questions because you cannot ask such a question experimentally*". In any case, even today, it remains true that no experimental result has been found to be in

disagreement with standard QM yet. Moreover, it can be noticed that the successes of QM are so numerous and its predictions so accurate that, from the computational point of view, no comparable scientific theory has ever existed. So, it is obvious, that all previous criticism were therefore directed against the interpretation of the theory but not against its practical validity.

2.1.2.- The De Broglie-Bohm's interpretation of quantum mechanics

Those physicists who did not accept the 'final' version of QM disagreed with the philosophy of the Copenhagen school in particular in one point: they thought that it was possible and useful to complete the theory in such a way as to make it causal. In other words, there is something more in the real world that is not contained in the wavefunction description (i.e. hidden variables) that allows us, for example, to talk of position and momentum simultaneously even if they are not simultaneously measurable. However, in 1932 John Von Neumann proposed his famous theorem establishing the impossibility of a causal completion of QM [Von Neumann 1955]. Bohr, Born, Pauli, Heisenberg stressed the importance of this theorem, and the great authority of these physicists, together with the mathematical complexity of Von Neumann's theorem, had the practical effect of outlawing the idea of hidden variables. From 1935 to about 1970 the physicists who worked on the problem of causality were indeed few and far between. Notwithstanding this, important results were obtained by Bohm (1952) and by de Broglie (1960), who managed to do what von Neumann had declared impossible: *find a hidden-variable model that does not contradict quantum mechanics in its statistical predictions and, at the same time, provides a causal foundation for the individual behaviour of single quantum systems.* It took some time before Bohm's and de Broglie's results were fully appreciated. In fact, until it was understood that von Neumann's theorem, although mathematically correct, could in no way forbid deterministic generalizations of QM, for the simple reason that one of its axioms was in general not physically reasonable.

In particular, Bohm showed conclusively that one could analyse the causes of individual atomic events in terms of an intuitively clear and precisely definable model. This model ascribe physical reality to magnitudes such as position and momentum independently of the observation. At the same time, this model reproduce all experimental predictions of standard QM. In this regard, Bohm's formulation retains the concept of wavefunction from the standard QM and postulates the existence of particles.

The basic postulates of the BB interpretation are[Holland 1993]:

- (1) An individual physical system comprises a wave propagating in space and time together with a point particle which moves continuously under the guidance of the wave.
- (2) The wave is mathematically described by the wavefunction, $\Psi(x,t)$, solution of the Schrödinger equation.
- (3) The particle motion is obtained as the solution $x(t)$ to the equation:

$$v(x,t) = \frac{dx(t)}{dt} = \frac{1}{m} \nabla S(x,t) \Big|_{x=x(t)} \quad (2.1)$$

where $S(x,t)$ is the phase of the wavefunction. To solve this equation we have to specify the initial position $x(0)=x_B$.

These three postulates constitute a consistent theory of motion. In order to ensure the compatibility of the motions of the ensemble of particles with the results of QM, a further postulate is needed:

- (4) The probability that a particle in the ensemble lies between the points x and $x+dx$ at time t is given by:

$$R^2(x,t) \cdot dx^3 \quad (2.2)$$

where $R(x,t)=|\Psi(x,t)|$

This postulate has the effect of selecting from all the possible motions implied by the law (2.1), those that are compatible with an initial distribution $R^2(x,0)=|\Psi(x,0)|^2$. We will show later that, with these postulates, the standard results of QM are perfectly reproduced in terms of single particle trajectories. Apart from this, the BB approach provides a deeper structure to QM that avoids the obscure interpretation of the QM measurement with the wavefunction collapse. In this regard, as Bohm trajectories have a physical reality independently of the measurement, they are intuitively clear for our minds.

At this point, following the Bohm's original paper [Bohm 1952], it will be interesting to mathematically deduce how the Schrödinger equation can be rewritten to obtain causal trajectories. We start by rewriting the wavefunction in polar form:

$$\psi(x,t) = R(x,t) \exp\left(i \frac{S(x,t)}{\hbar}\right) \quad (2.3)$$

where $R(x,t)$ and $S(x,t)$ are two real functions representing, respectively, the modulus and phase of the wavefunction. Then, if we substitute $R(x,t)$ and $S(x,t)$ into the time dependent Schrödinger equation, we can split it into two real equations by separating the real and imaginary parts. The real part leads to the following equation:

$$\frac{\partial S(x,t)}{\partial t} + \frac{1}{2m} \left\{ \frac{\partial S(x,t)}{\partial x} \right\}^2 + V(x,t) - \frac{\hbar}{2m} \frac{1}{R(x,t)} \frac{\partial^2 R(x,t)}{\partial x^2} = 0 \quad (2.4)$$

that can be interpreted as a generalized Hamilton-Jacobi equation assuming that the momentum is described by the spatial derivative of the phase:

$$\frac{\partial S(x,t)}{\partial t} + H \left[x, \frac{\partial S(x,t)}{\partial x}, t \right] = 0 \quad (2.5)$$

where the Hamiltonian in addition to the kinetic energy and to the classical potential $V(x,t)$, contains a new term $Q(x,t)$, called the quantum potential:

$$Q(x,t) = - \frac{\hbar}{2m} \frac{1}{R(x,t)} \frac{\partial^2 R(x,t)}{\partial x^2} \quad (2.6)$$

Within the BB approach, this new potential term correctly accounts for all the differences between classical and quantum dynamics. In particular, $Q(x,t)$ introduces the non-local features characteristic of quantum phenomena. Obviously, when $Q(x,t)$ is negligible compared with the other relevant energy terms, classical trajectories are obtained.

Equivalently, the imaginary part of the Schrödinger equation gives an equation for $R(x,t)$:

$$\frac{\partial R^2(x,t)}{\partial t} + \nabla \left(\frac{1}{m} \frac{\partial S(x,t)}{\partial x} \cdot R^2(x,t) \right) = 0 \quad (2.7)$$

which can be identified as the continuity equation because $R^2(x,t)$ is the presence probability density (postulate 4) and the expression inside the gradient can be mathematically demonstrated to be identical to the standard definition of the current density.

At this point, we need to discuss how the Heisenberg's uncertainty principle is compatible with this causal formulation of QM. Although a single Bohm trajectory has no uncertainties on its dynamic magnitudes, any quantum system has an experimental uncertainty when a real experiment is carried out. Therefore, from a practical point of view, one can not know with absolutely accuracy which is the initial condition of the experiment (position, energy...). In this regard, an initial position probability distribution,

$R(x,0)=|\Psi(x,0)|^2$, has to be chosen for the simulation of experimental results. So, different Bohm trajectories (departing from different initial positions $x(0)=x_B$) have to be simulated. And as a consequence, within the BB, only average results are obtained in experiments. In other words, Heisenberg's uncertainties are not intrinsic to the BB interpretation (as it is in the standard one), but only due to experimental limitations.

In figure 2.1 we reproduce the work of Philippidis, Dewdney, and Hiley [Philippidis 1979] who showed in particular how a detailed calculation of the quantum potential for the usual two-slit experiment can give rise to interference without the need to abandon the notion of a well-defined particle trajectory. Their result shows that every particle follows a well-defined trajectory and that, in spite of this, the interference pattern is obtained since the particle probability density remains equal to $|\Psi(x,t)|^2$ for all times. This work is charged with philosophical implications for those who believed that the double-slit experiment did not allow any simple ('intuitive') explanation. In the words of Bell: "*De Broglie showed in detail how the motion of a particle, passing through just one of two holes in screen, could be influenced by waves propagating through both holes. And so influenced that the particle does not go where the waves cancel out, but is attracted to where they cooperate. This idea seems to me so natural and simple, to resolve the wave-particle dilemma in such a clear and ordinary way, that it is a great mystery to me that it was so generally ignored*" [Bell 1987]

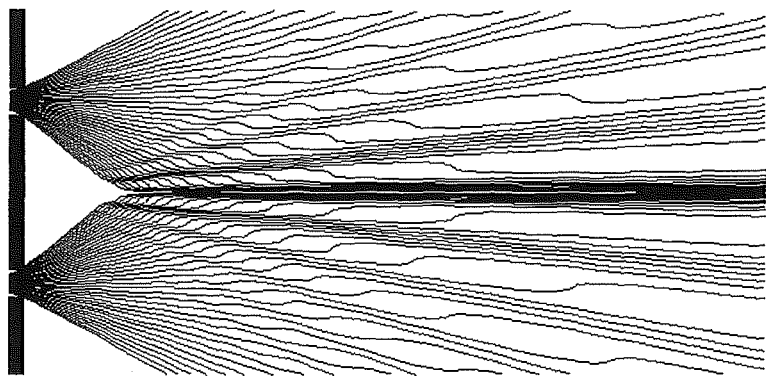


Fig 2.1: Particle trajectories for the double-slit experiment as calculated by Philippidis, Dewdney, and Hiley [Philippidis 1979]

Let us stress that, consistently with the Bohm's interpretation, but without invoking the generalized Hamilton-Jacobi theory or the quantum potential, all the dynamic behaviour of Bohm trajectories can be equivalently obtained

by defining the particle velocity, described by the $\Psi(x,t)$, with the quite classically-intuitive expression:

$$v(x,t) = \frac{1}{q} \frac{J(x,t)}{|\Psi(x,t)|^2} \quad (2.8)$$

where q is the absolute value of the electron charge.

At this point, once more, we want to stress how the standard QM results can be exactly reproduced in terms of individual trajectories. Following the Bohm's formulation, the initial position is uncertain and only the presence probability density $|\Psi(x_B,0)|^2$ is considered to be known at $t=0$. So, the physical observables $\langle A \rangle$ must be computed by averaging the corresponding magnitude $A(x_B,t)$ over all possible Bohm trajectories [Leavens 1993]:

$$\langle A \rangle = \frac{\int_{-\infty}^{\infty} A(x_B,t) |\Psi(x_B,0)|^2 dx_B}{\int_{-\infty}^{\infty} |\Psi(x_B,0)|^2 dx_B} \quad (2.9)$$

In particular, as a direct consequence of the continuity equation, the presence probability density at an arbitrary position x can be recovered by 'counting' all the particles:

$$|\Psi(x,t)|^2 = \int_{-\infty}^{\infty} dx_B |\Psi(x_B,0)|^2 \delta(x - x(x_B,t)) \quad (2.10)$$

and the current density by weighting their velocities:

$$J(x,t) = q \int_{-\infty}^{\infty} dx_B |\Psi(x_B,0)|^2 v(x,t) \delta(x - x(x_B,t)) \quad (2.11)$$

From the above two expressions, avoiding any physical interpretation, the BB approach can be exclusively considered as a mathematical tool which is able to reproduce the presence probability and current density associated to $\Psi(x,t)$ using well defined particle trajectories. Moreover, since the main goal of any device simulator is to obtain charge densities (i.e. self-consistent potential profiles) and current fluxes, the two previous equations demonstrate that we can obtain reliable results using Bohm trajectories and treat the classical and quantum regions equivalently.

2.1.3.- Additional information provided by the De Broglie-Bohm interpretation.

We have stressed that Bohm trajectories exactly reproduce the measurable results obtained with standard QM. However, Bohm's interpretation also provides other results that do not have a counterpart within the standard framework of QM. This is not surprising since the causal trajectories give a deeper structure to the quantum theory. An example of the nonconventional information provided by the BB approach is the case of tunneling times (a detailed discussion of different approaches for the description of tunneling times is found in [Hauge 1989] and [Landauer 1994]). In particular, Leavens have devoted a lot of work to study these times within the BB interpretation [Leavens 1993]. Since the Copenhagen interpretation of QM denies the probability of talking about trajectories, the answer to the question: "*How much time does the electron take to traverse the barrier?*" is a nonsense (in Bohr's words, you can not ask this question experimentally). However, when the quantum formalism is regarded from Bohmian mechanics, these paradoxes or perplexities (so often associated to with quantum philosophy) simply evaporate. Following these steps, we have also studied the implications of the noncrossing properties of Bohm trajectories in the practical computation of these times in double barrier potential profiles [Paper D].

In particular, when RTD are involved, it seems natural that one needs to speak about the time that an electrons takes to traverse the double barrier (directly related with its high frequency application). However, although these concepts are natural in the BB interpretation, they are part of the *unspeakable quantum mechanics* (i.e all additional results that have not an analogue within the standard interpretation of QM, should be regarded with caution until Bohm's theory is confirmed or refuted by experiments). In any case, in the present thesis, this hidden information is considered as a byproduct that can be useful to enlighten some obscure fields in quantum transport. Let us express our opinion using Fischetti's words: *We need to keep an open mind: Otherwise surprises (and discoveries) would never happen.*

Finally, let us point out that, although recent experiments on quantum teleportation evidence, once more, that the discussion about "locality" and "realism" in QM is far from resolved [Furusawa 1998], the present thesis does not contribute to this discussion.

2.2.- Properties of Bohm trajectories

Following the goal of providing a classical intuitive picture for electron tunneling, the present section is devoted to study how Bohm trajectories can

describe the mesoscopic electron transport in RTD. First of all, we will discuss two relevant characteristics of Bohm trajectories.

It is widely assumed that intuition is a very important issue for our understanding of nature. It is in this regard that it can be said that the Copenhagen interpretation of QM remains impossible to be understood within a classical framework. But, as intuition is unavoidably subjected to a cultural environment, it is argued that once you have grown with concepts such as wavefunctions, quantum jumps, nonlocality or wave-particle dualism, you may find it intuitive (i.e. you can build a mental picture of what goes on and make predictions about how a physical system will behave). In any case, as far as electronic transport in mesoscopic devices is concerned, a classical intuitive picture is an unquestionable advantage for any simulation tool. In our opinion, aside from the quantum philosophical objections, Bohm trajectories can provide a common language (intuitive picture) for people working with mesoscopic devices (from theoretical physicists to device modeling engineers).

On the other hand, we want to stress that, in addition of being intuitively appealing, Bohm trajectories exactly reproduce the observable results of standard QM by construction. In other words, the QM information present in the wavefunction is equivalently contained in the Bohm trajectories dynamics. The function used to describe the quantum system determines how Bohm trajectories behave. In this regard, we will study Bohm trajectories associated to either pure or mixed states.

In particular, we are interested in describing a constant flux of electron in double barrier potential profile. First, we will consider that this quantum system is described by an eigenstate $\phi_k(x)$. But finally, after using a time dependent wavepacket $\psi(x,t)$, we will show that an incoherent superposition of wavepackets $\rho_{kk'}(t)$ (i.e. a particular kind of the density matrix described in 1.3.2) perfectly fits with our goal for building a Quantum MC simulator. In all the cases, we will evidence that any complain related with a particular counterintuitive behaviour of Bohm trajectories can also be directly imputed to the associated function model

2.1.2.- Bohm trajectories associated to time-independent states

Let us assume that an electron is described by a time independent wavefunction $\phi_k(x)$ solution of the Schrödinger equation. These states are associated with a constant flux of particles, so it seems natural that the probability presence does not change with time. However, let us wonder about the meaning of the dynamic information that they provided. In this regard, let us compute Bohm trajectories associated to these states.

Because of the monoenergetic description of $\varphi_k(x)$, Bohm trajectories associated to these states can be easily computed. In particular, $\partial S(x,t)/\partial t = -E_k$, so that, equation (2.4) can be rewritten as a energy conservation law:

$$E_k = V(x) + Q(x) + \frac{1}{2}mv(x)^2 \quad (2.12)$$

The quantum potential $Q(x)$ depends only on the modulus of the wavefunction, and hence, it has no dependence on time. Moreover, as the classical potential $V(x)$ is also time-independent, the velocity of all different Bohm trajectories have only one possible value at each position, $v(x)$, that do not depend on time. (i.e. there is a unique trajectory in the phase space) [Paper C].

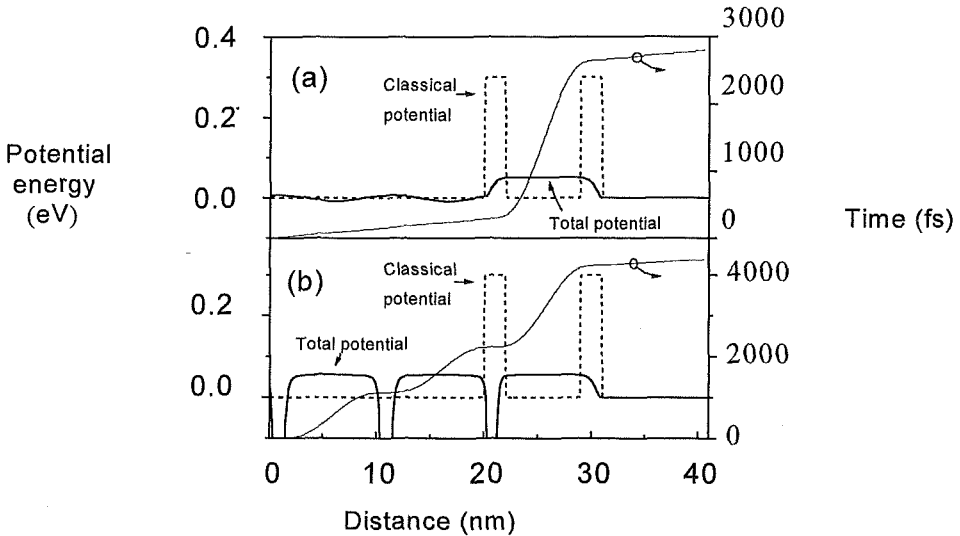


Fig. 2.2: Bohm trajectories associated to stationary scattering states impinging on a typical GaAs/AlGaAs RTD with 2 nm barriers of 0.3 eV separated by a 7 nm well. The classical potential and the total potential (the sum of classical and quantum terms) are also depicted in dashed and solid lines, respectively. (a) Resonant eigenstate, $E_k=0.05$ eV; (b) Non-resonant eigenstate, $E_k=0.06$ eV.

As an example, let us concentrate on extended states travelling from left to right. These states represent a constant flux of particles, incident upon a barrier, partially transmitted and reflected. For these states, the current density is position independent and the probability presence is extended to the whole device. So, Bohm trajectories can depart from all positions and the

standard current and charge density values are perfectly reproduced. In Fig. 2.2(a) we have represented one of these trajectories for a state incident from left to right upon a potential profile of a typical RTD. Its energy $E_k=0.05$ eV corresponds to the first resonant level of a GaAs/AlGaAs. In this particular case, where the transmission coefficient $T(k)$ is very close to unity, the results obtained within the Bohm's approach are quite compatible with our intuitive understanding of the tunneling phenomenon: all particles are transmitted and the particle velocity decelerates in the well.

Counterintuitive results associated to time independent states

However, the situation is far from clear for non resonant states. In Fig. 2.2(b), we have represented one of these non-resonant trajectories for the same potential profile. Although $T(k)$ is much smaller than unity for the non-resonant states, they present the same features as the resonant ones: all Bohm trajectories are transmitted through the barrier. This fact can be easily understood from a mathematical point of view. Apart from using equation 2.12, the particle velocity can be equivalently computed as the quotient between current and probability presence densities (eq. 2.8). For these states, both densities are time-independent and positive everywhere. So, the Bohm velocity is always positive. In this regard, although Bohm trajectories associated to scattering states perfectly reproduce the presence probability and the current density, they do not reproduce our particle-intuitive understanding of the tunneling phenomenon since, in principle, we would expect to find reflected as well as transmitted trajectories.

However, we can not conclude that Bohm's approach fails for scattering states. As we have said in the introduction of the present section, Bohm trajectories exactly reproduce the dynamic information contained in the wavefunction. In our opinion, the problem resides in the fact that extended states describe a constant flux of incident and reflected electrons:

$$\varphi(x,t) = \left\{ \underbrace{\frac{1}{2\pi} e^{ikx}}_{\text{incident}} + \underbrace{\frac{1}{2\pi} r(k) \cdot e^{i(-k)x}}_{\text{reflected}} \right\} e^{i\frac{E_k}{\hbar}t} \quad (2.13)$$

As a consequence, the velocity of Bohm particles is neither related to the incident electron nor the reflected one, but to the average of both. In particular, if the barrier is infinitely high, then the reflection coefficient is equal to one and Bohm's velocity is zero (one would expect positive and negative electron velocities simultaneously). This argumentation is consistent with the first example: if the reflected plane wave is not present (the transmission coefficient equal to unity), then, Bohm trajectories reproduce our intuitive picture for tunnelling.

Another example of the unphysical results obtained from Bohm trajectories is the oscillatory behavior of the velocity in the emitter (as is seen in figure 2.2). Obviously, this oscillatory behaviour is due to the oscillatory behaviour of the probability presence density in the emitter region, however, its quite difficult to justify why an electron situated very far from the barrier, will find some prohibited region (i.e. $|\varphi_k(x)|^2=0$). For a detailed discussion of this unphysical behavior of Bohm trajectories see [Paper C] and [Paper D].

Our intuitive picture for tunneling is based on the fact that the electron is first incident and then, after a time, reflected. In conclusion, we can said that although these extended states can be useful (as a complete base) for describing macroscopic variables of the device (charge and current), they have serious counterintuitive aspects when used to describe the dynamics of particle tunneling.

2.2.2.- Bohm trajectories associated to time-dependent wavepackets.

For the Monte Carlo simulation based on Bohm trajectories, we need a time dependent description of tunneling. In this regard, we can consider that an electron is described by a time dependent wavepacket, $\psi_{k_c}^0(x,t)$, whose initial boundary condition, (at $t=t_0$) is a Gaussian wavepacket (i.e. a wavepacket with a minimum position uncertainty):

$$\psi_{k_c}^{t_0}(x, t_0) = \frac{1}{(\pi\sigma_x^2)^{1/4}} \exp\left(-\frac{(x-x_c)^2}{2\sigma_x^2} + ik_c x\right) \quad (2.14)$$

σ_x being the spatial dispersion, x_c the spatial center of the wavepacket at time $t=t_0$, and k_c the centroid of the wavevector distribution which is related to a central energy E_c . For reason that will become evident later, we define t_0 as minimum spatial uncertainty time and we use it. t_0 label the wavepacket. In other words, t_0 is the time when the wavepacket has its minimum spatial uncertainty. From a practical point of view, $\psi_{k_c}^{t_0}(x,t)$ is computed by a superposition of Hamiltonian eigenstates as described in equation 1.3. The complete algorithm to compute the wavepackets is explained in [Paper C]. Then, the velocity of Bohm trajectories, at any time and position, is computed as the quotient between current and presence probability densities (eq. 2.8). Contrarily to the Hamiltonian eigenstates, since the velocity of Bohm trajectories associated to a wavepacket depends also on time, there are different Bohm trajectories in the x-t plane.

In Fig. 2.3 we show several of these trajectories corresponding to the second transmission resonance ($E_c=0.22$ eV) of the structure described in the figure. All Bohm trajectories are associated to the same wavepacket. They depart at $t=t_0$ from any position x_B according to the initial gaussian distribution $|\psi_{k_c}^{t_0}(x_B, t=t_0)|^2$. The observable results obtained from this ensemble of Bohm trajectories, perfectly reproduce the standard QM results. The trajectories coming from the front of the wavepacket are transmitted, while those from

the rear are reflected (most of them without even reaching the barrier). This is caused by the fact that Bohm trajectories do not cross each other in configuration space [Paper D]. If the barrier region is limited by $x_L < x < x_R$, we can calculate the wavepacket transmission coefficient $T(k_c)$ by computing the probability presence at the right of point x_R for $t \rightarrow \infty$. Moreover, we can also computed $T(k_c)$ by counting all the transmitted particles:

$$T(k_c) = \int_{x_R}^{\infty} |\Psi_{k_c}^{to}(x, t \rightarrow \infty)|^2 dx = \int_{-\infty}^{\infty} \alpha_T(x_B) |\Psi_{k_c}^{to}(x_B, t_0)|^2 dx_B \quad (2.15)$$

where $\alpha_T(x_B)$ is equal to unity if the particle is transmitted and zero otherwise.

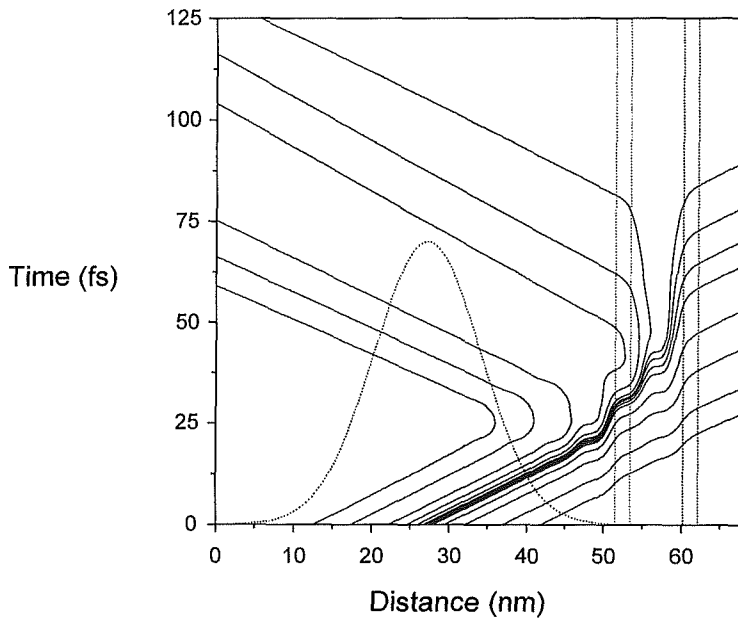


Fig. 2.3: Bohm trajectories associated to an initial Gaussian wavepacket with a central energy of 0.22 eV and a spatial dispersion of 10 nm, impinging upon a double barrier structure with 2 nm barriers of 0.3 eV and 7 nm well. The barriers and the initial Gaussian wavepacket are indicated by dashed lines.

Let us remind that it was not possible to reproduce the transmission and reflection coefficient of stationary extended states by counting transmitted Bohm trajectories (all particles were transmitted for extended states). Finally, let us said that some practical implications of the non crossing properties of one dimensional Bohm trajectories are explained in detail in [Paper D]. Other general observations about Bohm trajectories in time dependent wavepackets can be found in [Paper E] and [Paper F].

From the behavior of the trajectories shown in Fig. 2.3, one could conclude that the intuitive picture of particles bouncing back and forth inside the well at resonance (as in a Fabry-Perot interferometer) is not reproduced by the Bohm trajectories. However, this conclusion is not exactly correct, since oscillating trajectories are indeed found in other situations (i.e. different parameters for the potential and/or the wavepacket). In general, we can confirm that Bohm trajectories oscillate whenever the wavepacket oscillates between the barriers (see [paper C] for a detailed discussion of the oscillatory behavior of Bohm trajectories). In conclusion, as it has been repeatedly stressed, Bohm trajectories are a perfectly equivalent alternative to the wavefunction for the description of the electron dynamics.

Uncertainties and counterintuitive results with time dependent states

Although, Bohm trajectories associated to time evolving wavepackets seem to provide an accurate intuitive picture of tunneling, there are also some physical objections when electrons are described by these states.

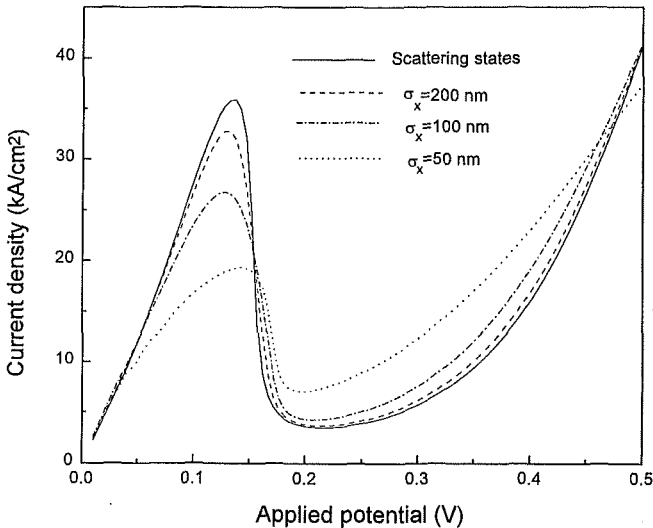


Fig 2.4: Non-selfconsistent I-V curves for a typical RTD computed using scattering states or initial Gaussian wavepackets with different values of its spatial dispersion σ_x .

First of all, the spatial dispersion, σ_x , which determines the initial spatial dimensions of the electron, remains undefined and an *ad hoc* criterion are required for its selection. In figure 2.4, we show how the choice of σ_x determines the simulated macroscopic performance of the device: four different non-selfconsistent I-V curves are obtained for four different spatial dispersion of the wavepackets. In informal words, we can say that there is not an easy answer to the question: “Which is the spatial extension of the electron?” in the sense formulated by Fischetti [Fischetti 1998].

On the other hand, the spreading of a time dependent wavepacket has no counterpart in classical electronic transport. For an initial Gaussian wavepacket in a flat potential, the centre of mass of the wavepacket moves like a particle that obeys the laws of classical mechanics. On the other hand, it is already well known that, while the momentum dispersion is a constant of motion, the spatial dispersion of the wavepacket varies with time and, for sufficiently long times, increases without limit (spreading of a wave packet, see [paper H]). This classically unintelligible phenomenon is not limited to the special initial Gaussian wavepacket, but to any arbitrary free wavepacket [Cohen-Tanoudji 1977].

2.2.3.- Bohm trajectories associated to the density operator

For building up our Monte Carlo simulation, we are interesting in providing an adequate description for a constant flux of electrons moving inside the RTD device. When discussing Hamiltonian eigenstates we notice that they 'seems' to provide an accurate description for a constant flux of particles (i.e. they are time independent and their presence probability extends along the whole device). However, we have clearly notice that their dynamic information is unsatisfactory. On the other hand, a single wavepacket, although containing reliable dynamic information, it can not provide a picture of a flux of electrons.

In this section, following the idea of providing a function model to describe a flux of picture with reliable time dependent information, we will a specific density operator. This particular density operator is build up as an incoherent sum of wavepackets that, as we will see, contains the dynamic information of the wavepackets while maintaining the stationary properties. (i.e. this density matrix will be shown to be time independent and its associated presence probability extends along the whole device like Hamiltonian eigenstates).

Before defining it, let us develop a simpler expression for the density matrix of a single wavepacket. As we have said, when all information about the quantum system is known, it can be equivalently described by the Schrödinger or Liouville equations. In particular, using the notation of equation 1.4, the density matrix for a single wavepacket can be written as:

$$\rho^{o_{k'k}}(t) = \langle \varphi_{k'} | \psi(t) \rangle \langle \psi(t) | \varphi_k \rangle = a(k') a^*(k) e^{\frac{(E(k) - E(k'))(t - t_0)}{\hbar}} \quad (2.16)$$

let us notice the presence of the parameter t_0 called the minimum-uncertainty time

As we have said, for our quantum MC simulator, we are interested in modelling a constant flux of electrons. We can model this picture by considering simultaneously (emphasis on simultaneously) lots of identical wavepackets that have arrived at the region of interest at different times. All these wavepackets are defined by equation 2.14 with the same wavepacket parameters (i.e. identical central energy E_c , identical spatial dispersion σ_x and identical central position x_c). However, since each wavepacket have arrived at a different time, it have reached (or will reach) it minimum spatial uncertainty at a different time t_0 . In other words, each wavepacket of the system can be labelled by its t_0 value. From a mathematical point of view, this quantum system can not be represented by a coherent superposition of wavefunction, but by an incoherent sum of them (i.e. the density matrix formalism has to be used). In this regard, the whole electron ensemble can be written taking into account (2.16) and a sum over all possible entering times, t_0 . If we suppose that the minimum-uncertainty time is uniformly distributed from $-\infty$ to $+\infty$ (i.e, $f_n=1$ for expression 1.4) , then:

$$\rho_{kk'}(t) = \int_{-\infty}^{\infty} \rho^{(t_0)}_{kk'}(t) \cdot dt_0 = \int_{-\infty}^{\infty} a(k')a^*(k)e^{i\frac{(E(k)-E(k'))(t-t_0)}{\hbar}} \cdot dt_0 \quad (2.17)$$

In order to clarify our definition, let us represent this function for a typical double barrier RTD. We have selected wavepackets with a central energy $E_c=0.1$ eV, a spatial dispersion of $\sigma_x=10$ nm and central position $x_c=60$ nm. At any particular time, there are lots of different wavepackets evolving in the system. Some of them have already arrived at its minimum uncertainty position, but others have not passed through it yet. In figure 2.5 we have represented the probability presence of finding an electron associated to the density matrix described by equation (2.17). In this regard, each horizontal line represents the probability presence of a particular wavepacket (the wavepacket that at $t=t_0$ has its minimum uncertainty). On the other hand, each vertical line represents an additional probability distribution, $f(t_0)$. At each position, the probability of finding the electron can be decomposed into a t_0 -distribution. In other words, if the exact position of the electron is determined, an uncertainty about which is the t_0 -wavepacket associated to the electron remains. Finally, let us mention that in figure 2.5 the t_0 -information is still 'alive' because the t_0 -integral in (2.17) is not evaluated. In this regard, since ρ depends only on $t-t_0$, the expression (2.17) will take identical values either considering the intervals [t fixed, $-\infty < t_0 < \infty$] or [$-\infty < t < \infty$, t_0 fixed]. This means that the roles of t and t_0 are interchangeable. Figure 2.5 can also be interpreted in a quite different and simple way. It can also represent the probability presence distribution of a single t_0 -wavepacket evaluated for different times t . In this regard, in spite of its dynamic origin, the function can be defined, somehow, as stationary.

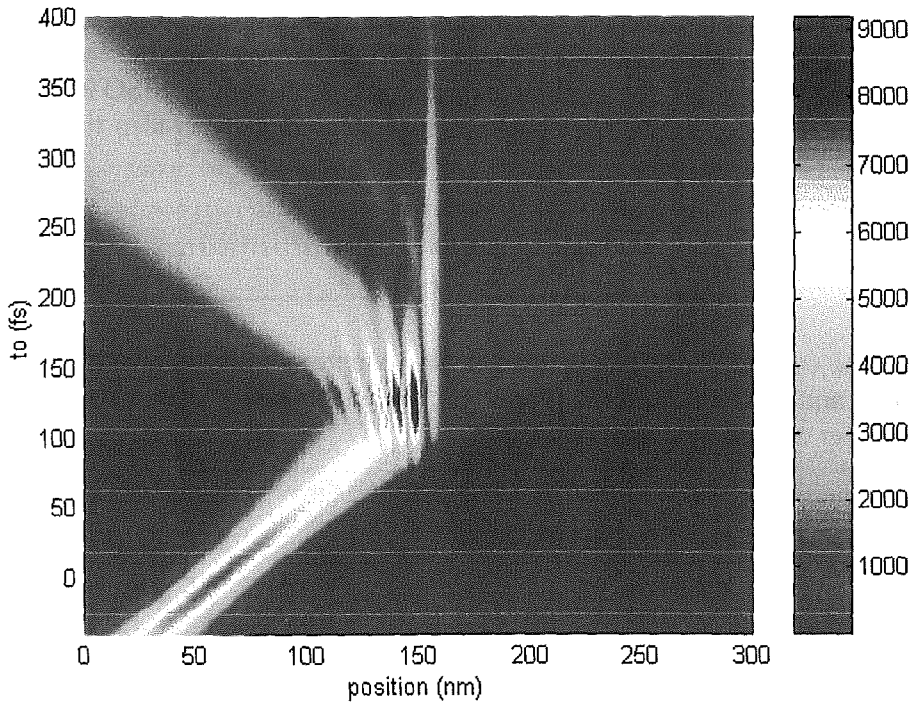


Fig 2.5: representation of a SISOW in a x - t_0 space. The wavepackets that define the SISOW have a central energy $E_c=0.1$ eV, a spatial dispersion of $\sigma_x=10$ nm and central position $x_c=60$ nm. Each horizontal line is the probability presence of one of the wavepackets evaluated at a particular t_0 .

In particular, if we use the identity:

$$\frac{1}{2\pi} \int_{-\infty}^{\infty} e^{i \frac{(E(k)-E(k'))t_0}{\hbar}} dt_0 = \frac{m^*}{\hbar} \frac{1}{k} \{\delta(k-k')\} \quad (2.18)$$

then, we find that each element of the density matrix can be rewritten as:

$$\rho_{k',k}(t) = a(k')a^*(k)e^{i \frac{(E(k)-E(k'))t}{\hbar}} \cdot 2\pi \frac{m^*}{\hbar} \frac{1}{k} \delta(k'-k) \quad (2.19)$$

We notice that, even working with time-dependent wavepackets (rather than with Hamiltonian eigenstates), we have found a diagonal density matrix for our system when (2.17) is integrated along t_0 . In the next chapter, when we will explain our Monte Carlo procedure, we will assume that the flux of electrons, at each energy, is adequately described by this entity $\rho(t)$ that we will call Stationary incoherent superposition of wavepackets (SISOW).

Intuitive results with the SISOW representation

Once the SISOW density matrix is obtained, all the observable results can be obtained from it. In particular the charge and the current can be easily computed (See [paper H] for explicit expression). Although a SISOW is build up from time-dependent wavepackets, its charge density is also time-independent:

$$Q(x,t) = 2\pi \frac{m^*}{\hbar} \int_{-\infty}^{\infty} |\psi_k(x)|^2 \frac{|a(k)|^2}{k} dk \quad (2.20)$$

Moreover, the current density associated to this quantum entity is also time-independent and position-uniform [Paper H]. It can be easily demonstrated that the current carried by a SISOW is:

$$J(x,t) = \frac{\hbar}{m^*} \int_{-\infty}^{\infty} |a(k)|^2 T(k) dk \quad (2.21)$$

By defining $a(k) = \delta(k - k_c)$, one recovers the standard expression for the current density of scattering states: the current of a scattering state is proportional to its transmission coefficient. In figure 2.6 we have represented the charge associated to a stationary state (with energy near to the second resonance of the well 1.1 eV) to be compared with the charge associated to a SISOW with identical central energy and a spatial dispersion of 200 Å. We realize that the oscillatory behavior of the stationary state in the emitter, that has a quite embarrassing explanation, disappears when a SISOW is considered. Moreover, the spreading of the wavepacket does not have any importance since the SISOW is ‘spread’ everywhere like a time independent eigenstate.

The parameters needed to define a SISOW are obviously related to the ones needed to specify the wavepacket. In particular a SISOW is determined by the central energy E_c and the spatial dispersion σ_x . (It can be easily demonstrated that all results are independent of the initial central position x_c of the wavepacket provided that it is initially defined in a flat potential region). However, as it is seen in expression 2.20 and 2.21, the macroscopic results depend on $a(k)$ and, hence, on the spatial dispersion of the wavepackets. Nonetheless, as we have pointed out for the wavepacket, this is an advantage rather than a drawback, since it introduces some flexibility regarding the modeling of the “size of an electron”, in the sense described by Fischetti [Fischetti 1998]. In this way, regardless of technical or numerical difficulties, a SISOW can *a priori* be used to define either classical particles by using by considering $\sigma_x \approx 0$ (i.e. $a(k) \approx cte$), or also Hamiltonian eigenstates by considering $\sigma_x \approx \infty$ (i.e. $a(k) = \delta(k - k_c)$). Obviously, these two

limiting situations drive to quite different macroscopic results, as we have seen in figure 2.4 and 2.6.

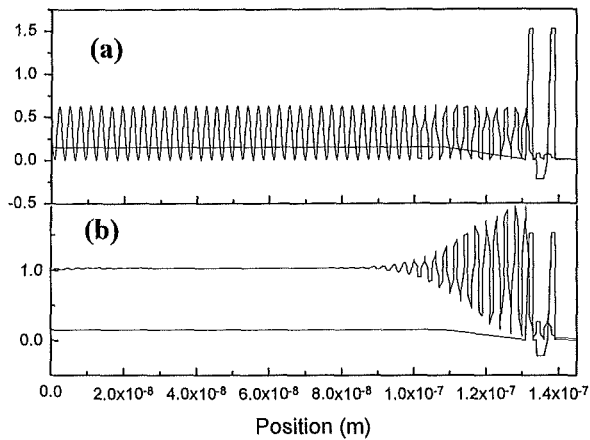


Fig 2.6: Probability distribution for: (a) stationary state and with an energy of 1.1 eV (b) a SISOW with the same energy. The oscillatory behaviour of the probability presence in the stationary state in the emitter disappears when a SISOW is considered.

Moreover, although a SISOW provides a stationary picture for the electronic transport, when dynamic aspects are considered, it does not have the counterintuitive results observed for stationary states. The Bohm trajectories associated to a SISOW are the Bohm trajectories associated to a time dependent wavepacket. Let us explain this point. As we have said, t_0 and t can be mathematically interchangeable. In this regard the trajectories of figure 2.3 can be interpreted twofold. On one hand, they can be interpreted as the t -time evolution of trajectories associated to a single wavepacket (i.e. we can consider $[-\infty < t < \infty, t_0 \text{ fixed}]$). On the other hand, figure 2.3 can also be interpreted as an instantaneous picture of the stationary trajectories associated to a SISOW (i.e. we can consider $[t \text{ fixed}, -\infty < t_0 < \infty]$). In this last interpretation of figure 2.3, at each time t and position x , we obtain a velocity distribution. (This result has to be compared with the result for a single wavepacket where only one perfectly defined velocity is obtained at time t and position x).

References

[Bell 1987] J.S.Bell, *Speakable and Unspeakable in Quantum Mechanics*, Cambridge U.P., Cambridge, England

- [Bohm 1952] D.Bohm, *A suggested Interpretation of the Quantum Theory in terms of "Hidden" variables I*, Phys. Rev., v:85, p:166
- [Bohr 1935] N.Bohr, Phys. Rev. v:48, p:696
- [Cohen-Tanoudji 1977] C. Cohen-Tanoudji, B.Diu, and F.Laloë, *Quantum Mechanics* Wiley, New York
- [Einstein 1935] A.Einstein, B.Podolsky and N.Rosen, Phys. Rev. v:47, p:777
- [Feynman 1963] R.Feynman, R. Leughton, M.Sands, *The Feynman lectures on Physics*, Addison-Wesley, Redding, Mass.
- [Fischetti 1997] M.V.Fischetti, *Theory of electron transport in small semiconductor devices using the Pauli master equation*, J. Appl. Phys., v:83(1), p:270
- [Furusawa 1998] A.Furusawa, J.L.Sorensen, S.L.Braunstein, C.A.Fuchs, H.J.Kimble, E.S.Polzik, *Unconditional quantum teleportation*, Science v:282 p:706
- [Hauge 1989] E.H.Hauge and J.A.Stovneng, *Tunneling times: a critical Review*, Rev. of Modern Physics, v:61(4), p:917
- [Holland 1993] P.R.Holland, *The quantum theory of motion*, Cambridge University Press, Cambridge
- [Landauer 1994] R.Landauer and T.Martin, *Barrier interaction time in tunneling*, Reviews of Modern Physics, v:66(1) p:217
- [Leavens 1993] C.R.Leavens and G.C.Aers, *Scanning tunnelling microscopy III*, (eds: R. Wiesendanger and M.J.Gütherodt). Springer, Berlin p:105
- [Philippidis 1979] C.Philippidis, C.Dewdney, B.J.Hiley, *Quantum interference and the quantum potential*, Nuovo Cimento v:52(B), p:15
- [Selleri 1990] F.Selleri, *Quantum paradoxes and Physical reality*, (Fundamental theories of physics) Kluwer Academic Press, The Netherlands
- [Von Neumann 1955] J.Von Neumann, *Mathematical Foundations of Quantum Mechanics*, Princeton University Press, Princeton

Chapter 3

QUANTUM MONTE CARLO SIMULATION

In this chapter, we present an explanation of our approach for the simulation of RTD. In particular, we explain its origin, its practical implementation and some significative results. See [Paper F] and [Paper G] for a complete explanation. First of all, since our proposal has many similarities with the classical MC technique, we will try to disclose why the MC technique is so useful in the simulation of semiconductor devices.

3.1. Classical Monte Carlo technique

The MC technique is a stochastic-numerical method that provides a solution of the BTE. This equation describes the evolution of the carrier distribution function, $f(x,k,t)$, inside a semiconductor device (without explicit quantum effects):

$$\frac{\partial f(x,k,t)}{\partial t} + v(k) \cdot \frac{\partial f(x,k,t)}{\partial x} + \frac{qF}{\hbar} \nabla_k f(x,k,t) = \left(\frac{\partial f(x,k,t)}{\partial t} \right)_{scattering} \quad (3.1)$$

where $v(k)$ is the electron velocity, F the external electric field and q the electronic charge. Along this work we will assume that the electrons are the only significative carriers in the RTD under study. The right-hand term, called the collision integral, can be rewritten as:

$$\left(\frac{\partial f(x,k,t)}{\partial t} \right)_{scattering} = \int \sum_i (S_i(k',k) \cdot f(x,k',t) - S_i(k,k') \cdot f(x,k,t)) \cdot dk \quad (3.2)$$

$S_i(k,k')$ being the probability per unit time for a transition from a state with wavevector k to another with k' due to the i -th scattering mechanism. Generally, $S_i(k,k')$ is computed using the familiar form of the Fermi's Golden rule in the first-order QM perturbation theory:

$$S_i(k',k) = \frac{2\pi}{\hbar} |M_i|^2 \cdot \delta(E(k) - E(k')) \quad (3.3)$$

where M_i is the matrix element of each of the interaction mechanism and $E(k)$ the energy of an electron with wavevector k [Cohen-Tanoudji 1977]. So, the BTE can be regarded as a differential-integral equation that only admits analytical solution for very few ideal cases. However, Chambers developed the BTE in a series expansion introducing a new set of mathematical variables $x(t), k(t), t$ [Chambers 1952]. What makes Chambers BTE version very interesting for electronic transport, is the fact that the new set of variables can be interpreted as physical magnitudes that describe a single particle trajectory. Between two scattering events the variables $x(t)$ and $k(t)$ evolve as follow :

$$\hbar \cdot k(t) = q \cdot F \quad \frac{d x(t)}{dt} = \frac{1}{\hbar} \frac{\partial E(k)}{\partial k} \quad (3.4)$$

In particular, if a parabolic relation is assumed between the electron energy and momentum, the electron trajectory, between successive scattering events, can be simply described by the classical Newton law: $m^* \cdot d^2 x(t) / dt^2 = q \cdot F$ where m^* is the electron effective mass (which takes into account the semiconductor band structure).

This intuitive picture for the description of the BTE perfectly fits with the basis of the MC simulation. In this particular case, the MC method for solving the BTE consists in evaluating $f(x,k,t)$ as an average over an ensemble of trajectories. Each electron trajectory is constructed as follow. First, a random number (distributed according to the transitions probabilities) determines the time (called the freeflight time) that the electron will evolve without collisions. After this time, other random numbers determine which is the involved scattering mechanism and also the final state after the scattering event. These two processes, repeated successively, perfectly define the electron trajectory [Gonzalez 1994].

The MC technique is usually called “the simulated experiment” because it directly provides an exhaustive dynamic information of all the carriers in the device. In this regard, the MC trajectories have surpassed their mathematical origin, to acquire the status of ‘real’ trajectories. Additionally, this ‘real’ role for the MC trajectories can be also justified within a simple QM environment. It is known that, if an electron is described by an initial gaussian wavepacket (solution of the Schrödinger equation), its central position and momentum also evolve following equation 3.4 when coherent

transport is assumed [Ashcroft 1976]. So, the MC trajectories can also be interpreted as physical entities that describe the QM dynamics in flat potential conditions without scattering.

The strength of the MC technique resides in the combination of an intuitive picture for the electrons with an accurate description for the simulation. Its introduction in the semiconductor environment is due to Kurosawa [Kurosawa 1966] who presented a study of high-field transport of holes in Ge. Its application to the simulation of electron devices started soon after, but it has only received great attention in the last two decades [Jacoboni 1989] due to the availability of the MC algorithms and computers needed to handle phenomena and systems of great complexity, much closer to the real devices. However, the BTE is not valid for the description of semiconductor devices where quantum effects are important (in particular, the BTE does not describe the electronic transport by tunnelling). So, as we have seen in section 1.3, other fundamental transport equations are required for the simulation of RTD. In this regard, the analytical formulation sketched by Chambers to interpret the BTE equation in terms of particle trajectories is also suitable for Quantum transport equations.

As we have said, none of the mentioned approaches in section 1.3 provides neither a simple algorithm nor an intuitive understanding of the quantum devices. The main goal of this work is to provide an extension of the classical MC simulation technique to deal with mesoscopic devices. Our approach pursues the consideration of the required QM effects while maintaining the intuitive appeal of the classical MC.

3.2.- A quantum MC simulator with wavepackets and Bohm trajectories

In order to explain our proposal, let us start by describing the different device regions that we consider in the simulator. We have divided the whole device in three regions: the emitter region, the quantum window QW where the potentials significantly change over distances of the order of the wavelength of the carriers, and the collector region (see fig 3.1). The electronic transport in the classical region (emitter and collector) is studied by means of the MC simulation of the Boltzman equation. On the other hand, inside the QW, we want to extent the concept of electron trajectory by using Bohm trajectories. In our model, the electron is pictured, consistently, as a point-particle along the whole device.

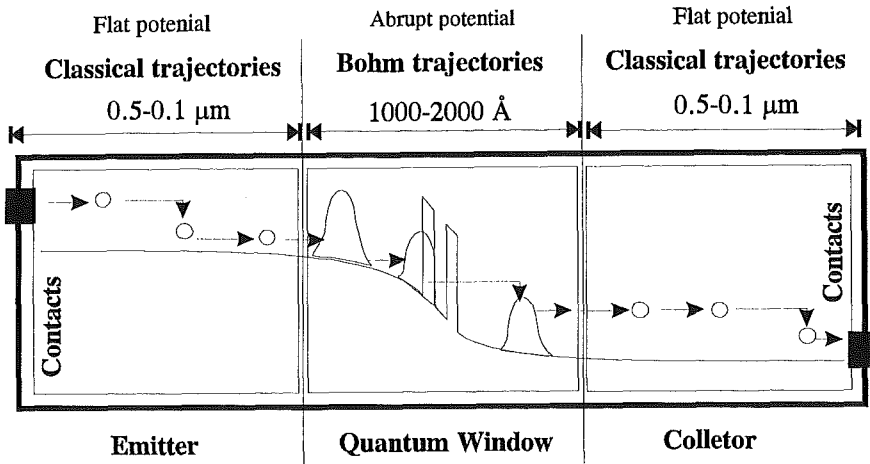


Fig 3.1: The device is divided into three regions: Emitter, Quantum Window(QW) and Collector. The Quantum MC method is applied at the QW where potentials change abruptly.

Basically, in figure 3.2 we have represented the four different procedures that describes how an electron ‘travels’ along the device. First, an electron enters inside the device by the classical contacts. Then, it evolves classically until it arrives at the QW. There, inside the QW, it moves following a Bohm trajectory. Either reflected or transmitted by the double barrier, the electron arrives at the classical region again and exits the device by the contacts. We have to model how the electrons enter/exit the device through the external contacts. Then, a standard classical MC model is needed for describing the electron trajectories in the emitter and collector regions. Finally, after defining the classical/quantum interface, we have to model how electrons move inside the QW.

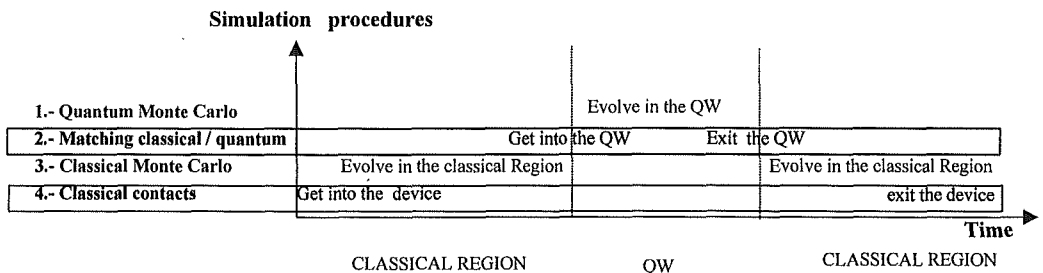


Fig 3.2: We describe the four simulation procedures that most electrons will suffer between entering and exiting the device.

Basically, the history of each electron that enters inside the device can be divided in these four simulation phases. Hereafter, we will explain them

devoting a special attention to the quantum MC and the quantum/classical matching description (which are the ones that support our quantum MC simulator proposal).

3.2.1.- Quantum Monte Carlo in the quantum region

Simplifying our proposal in order to provide a clear understanding of its implications, apart from the scattering mechanisms, the only difference between the classical MC and our quantum proposal is the way how we compute the carrier velocity. In the classical MC, the Newton law provides the carrier dynamics, while the Schrödinger equation (in Bohm's interpretation) has to be solved to compute the carrier velocity in the QW. Apart from this difference, as we will see, all others magnitudes such as current and charge densities are computed identically without differentiating between classical and quantum regions.

However, from a practical point of view, calculating the velocity within Bohm's approach requires a harder computing work (see equation 2.8). In order to be able to reproduce our intuitive picture (i.e time dependent process) of a particle impinging on a double barrier, we have to use a time dependent wavepacket in spite of a Hamiltonian eigenstate as we have stressed in the second chapter. In this regard, each electron inside the QW has to be associated to a particular Bohm trajectory associated to this wavepacket. Since electrons will arrive at the QW with different momenta, we have to be able to compute the time evolution of several different wavepackets, $\Psi_{k_c}^{t_0}(x,t)$ with different values of their central wavevector k_c and a minimum uncertainty time t_0 .

From a numerical point of view, as we have already explained, the practical computation of the wavepacket can be done in three steps. First, the time independent Schrödinger equation is solved to compute a set of Hamiltonian eigenstates, $\{\varphi_k(x)\}$. Second, the particular $a(k)$ values are calculated for the specific t_0 - k_c -wavepacket. And, finally, we use the superposition principle to compute the time evolution of all wavepackets (see equation 1.3). The main advantage of this method is that the wavepacket is computed at any arbitrary instant of time without having to calculate it at intermediate times. Details about the practical calculation of the set of Hamiltonian eigenfunctions, and the wavepacket k -components can be found in our papers [Paper C] and [Paper D].

Since the potential profile is modified at each time step of the MC procedure (ΔT) in order to reach self-consistence with the Poisson equation, all the eigenstates and wavepacket components must be recalculated after each ΔT . This means that at each time step, a table of (100x400) complex values have to be refreshed (which is the most significant additional effort needed to

incorporate Bohm trajectories in our MC simulator). Strictly speaking electrons that arrive at the QW are described by a SISOW. In particular, each electron inside the QW is associated to a particular k_c - t_0 -wavepacket, $\Psi^{k_c}_{t_0}(x,t)$ of the k_c -SISOW. Then, after choosing the initial conditions for each particle (i.e. x_B and t_B), its trajectory is computed by integrating the velocity (the velocity is computed by equation (2.8)).

Finally, let us said that in the present stage of the simulator we have not introduced the scattering between Bohm trajectories inside the QW, however, we will briefly discuss how this could be done in section 3.5.

3.2.2.- Matching classical/Quantum trajectories

Now, let us concentrate in explaining how the simple classical electron is reconverted to a quantum entity, and *viceversa*, at the boundaries of the QW. Basically, there are two points that we have to take into account to provide a good matching. First, we have to make compatible a classical and a quantum definition for an electron. A classical electron is perfectly described by a position, $x(t)$, and momentum, $p(t)$. However, a quantum electron is associated to wavepacket $\Psi^{k_c}_{t_0}(x,t)$ with an initial central position x_c , a constant central momentum k_c , a spatial dispersion σ_x and a minimum uncertainty time t_0 . Second, in order to be able to reproduce the standard QM results (point 4 in section 2.1.2), electrons have to be associated to Bohm trajectories that depart from x_B and t_B following the probability wavepacket distribution.

Let us discuss the first point. In principle, the classical electron momentum p is identified as the central wavepacket momentum, $p_c = \hbar k_c$. On the other hand, the x_c is fixed for all different wavepackets at specified position $x_c = x_L$ in the boundaries of the QW. However, the selection of σ_x is related with the discussion of section 2.2.3. If one wants to reproduce the standard Landauer-Büttiker results, then, a reasonable possibility is the choice of wavepackets wide enough in position ($\sigma_x \geq 25$ nm) so that the corresponding transmission coefficient is approximately that of the eigenstate associated to the central momentum, k_c (see fig. 2.4). Finally, the minimum spatial uncertainty time t_0 is related with the time that the electron enters into the QW.

Once the wavepacket parameters are selected (k_c , x_c , σ_x and t_0), a boundary condition for the electron (i.e a position, x_B , and t_B) has to be chosen to compute its trajectory. In order to be able to reproduce the wavepacket dynamics inside the QW, we only have to assure that x_B and t_B are selected according to the wavepacket probability presence. Next, we will explain two different models that achieve the previous requirement. In this regard, let us revisit the figure 2.5 used to describe the SISOW. We know that any horizontal line in the figure represents the probability presence of a particular wavepacket (i.e. a distribution function that depends on position x). So, when a particle arrives at the QW, we can fix its $t_B = t_0$ and determine its initial

position x_B according to the presence probability presence distribution (i.e according to $|\psi^{t_0}(x_B, t_0)|^2$). In figure 3.5, we have represented this model (that we call model A) where the darker square can qualitatively substituted by either figure 2.5 or 2.3.

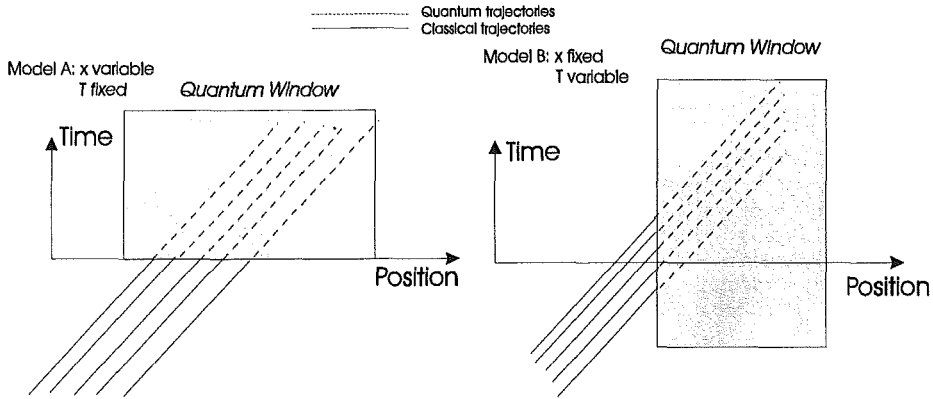


Fig 3.5: There are two possibilities to introduce Bohm trajectories inside the QW assuring that they will reproduce wave-function evolution. Model A: All particles depart from $t=t_0$ and from different initial position x_B , and Model B: All the particles depart from the same $x=x_B$ but they have different times t_0 . The darker squares can be qualitatively substituted by either figure 2.3 or 2.5.

On the other hand, we also know that any vertical line in the SISOW of the figure 2.5 represents a probability distribution that depends on t_0 , $f(t_0)$. So, when a particle arrive at the QW, we can fix its initial position $x_B=x_I$ and determine its initial time t_b according to this t_0 -initial probability distribution. We refer to this model by letter B (see fig 3.5). Both algorithms warrant that we will be able to reproduce the wavepacket dynamics inside the QW with Bohm trajectories. The model B has the technical advantage of being able to reduce the length of the QW, but we have to assure that all selected t_0 correspond to particles that enter inside the QW. Finally, we want to stress that the matching procedure is a crucial point in our simulator (in fact, any interface in MC simulations is always a problem). Moreover, in this interface, quite *ad hoc* models have to be unavoidably used to define any matching criteria because two quite incompatible different electron description are used.

3.2.3.- Classical Monte Carlo in the laterals regions

At this point, let us briefly present our classical MC algorithm. The electronic transport in the classical regions (emitter and collector), close to the respective contacts and characterised by smooth potential profiles, are

treated semiclassically. A conventional MC algorithm is used to simulate the particle dynamics. For simplicity, only the electronic transport in the lower valley with a constant effective mass has been taken into account (this approximation is also implicitly assumed in the QW where the Schrödinger equation is solved). The scattering mechanisms considered in these classical regions are: (i) Acoustic phonon scattering treated in the elastic approximation, (ii) polar optical phonon scattering and (iii) ionised impurity scattering. The transitions rates are calculated using the usual parameters for GaAs [Jacoboni 1989].

A detailed explanation of the Monte Carlo method and its practical implementation for their application to study electronic transport in conventional devices can be found in [Gonzalez 1993].

3.2.4.- Classical contacts

As any interface in MC simulation, as we have said, the problem of the boundary conditions for the BTE is not a trivial issue. Different models for the contacts are proposed in the literature. Among them, we will use the one developed by the MC group of Salamanca [Gonzalez 1996]. Basically, the procedure is as follow: if the cell adjacent to the contact is positively charged, carriers are injected from a velocity-weighted hemi-Maxwellian distribution at equilibrium until the cell is charge neutral. On the other hand, if the cell is neutral or negatively charged then, the number of particles in the cell is left unchanged.

3.3.- Simulated results for resonant tunneling diodes:

3.3.1.- Evaluation of macroscopic results

First of all, let us describe how the macroscopic results are obtained. As we have said, provided that Bohm trajectories are calculated as previously explained, they can be treated as classical trajectories for all purposes. Therefore, the same algorithms can be used to compute the charge and current densities in the QW or in the classical regions.

For example, at every time step ΔT the contribution of the i -th particle to the charge density of the n -th cell of width Δx_n is computed by evaluating the fraction of the time step spent by the particle in this cell, $t_i(n)/\Delta T$. An overall sum over the total number of particles N gives the electronic charge density associated to the specific cell:

$$C(n) = \frac{\sigma}{\Delta x_n} \sum_{i=1}^N \frac{t_i(n)}{\Delta T} \quad (3.5)$$

where σ is the charge per unit area represented by each simulated particle. At each time step, the obtained profile of the electronic charge density is used to update the potential by solving the Poisson's equation.

An identical procedure can be used to obtain the momentum distribution of the particles at each cell by using an additional momentum grid for each spatial cell. Since the exact position and momentum of each particle (even in the QW) can be perfectly defined, we can compute the time, $t_i(n,m)$, spent by the i -th particle in the phase-space cell (n,m) during the simulated time T . In this way, a time-averaged phase-space distribution $f_B(n,m)$ can be computed as:

$$f_B(n,m) = \frac{1}{T\Delta x_n \Delta k_m} \sum_{i=1}^N t_i(\Delta x_n, \Delta k_m) \quad (3.6)$$

Let us now discuss the meaning of this new phase-space distribution. In the classical regions, $f_B(n,m)$ is, by definition, a matrix representation of the BTE solution averaged over time $f(x,k)$. However, their meaning inside the QW is not so clear since the uncertainty principle makes, in principle, the definition of any phase-space distribution problematic. In any case, it is possible to establish a relationship between this phase-space distribution and the Wigner function, $f_W(x,p)$.

In particular, for a single wavepacket, it is known that the momentum computed by the Bohm's approach at each position, $f_B(x)$, is the mean value of the momentum of the Wigner distribution $f_W(x,p)$ [Muga 1993]:

$$f_B(x) = \left. \frac{\partial \mathcal{S}(x',t)}{\partial x'} \right|_{r'=r} = \frac{\int_{-\infty}^{\infty} p \cdot f_W(x,p) \cdot dp}{\int_{-\infty}^{\infty} f_W(x,p) \cdot dp} \quad (3.7)$$

In this regard, one can anticipate that both $f_B(n,m)$ and $f_W(x,p)$ will behave quite similarly when an ensemble of different wavepackets (i.e. a SISOW) is considered. In particular, it is very easy to demonstrate that the charge and current densities, that in both cases are computed as if they were classical distributions (i.e. a simple integral over the momentum distribution is done), give identical results. But, in spite of this relation, there is a fundamental difference (already pointed out in section 1.3.2) between the Wigner distribution and the Bohm's one: By construction, Bohm's phase-space distribution only takes positive values, while the Wigner function can also take negative ones and this obscures its physical interpretation (at least as a probability distribution).

On the other hand, the current along the device can be computed from the previous phase-space distribution. However, in order to avoid technical noise in the results, other equivalent methods can be used to compute the current. In particular under a constant applied voltage, the instantaneous current density $J(t)$ can be computed as the sum of the instantaneous velocities $v_i(t)$ of all the $N(t)$ particles contained in the device:

$$J(t) = \frac{\sigma}{L} \sum_{i=1}^{N(t)} v_i(t) \quad (3.8)$$

where L is the total simulated length of the device [Gruzinskis 1991]. By time averaging $J(t)$ one can obtain the stationary current for a given applied voltage.

3.3.2.- Simulated results

Hereafter, we will present some simulated results obtained with our quantum MC simulator in order to demonstrate the feasibility of our proposal. The steady-state I-V characteristic of a typical GaAs/AlGaAs double-barrier structure with 3 nm barriers of 0.3 eV and a 5.1 nm well has been simulated at 77 K. For simplicity, only one valley with an isotropic effective mass of $0.067m_0$ has been taken into account to model the conduction band. The ionised impurity density in the GaAs electrodes is $1.51 \cdot 10^{17} \text{ cm}^{-3}$, which corresponds to a realistic doping of $N_D = 5 \cdot 10^{18} \text{ cm}^{-3}$ at 77 K. The AlGaAs barriers and the GaAs well have been considered to be undoped. The total simulation length is 0.25 μm divided in 366 cells. The classical emitter (68.5 nm) and collector (96.5 nm) regions are divided into a non-uniform mesh, but the QW (84,9 nm) is divided into 283 constant cells of 0.3 nm each. Let us emphasise that the integration box is much larger than those typically used for solving the Liouville equation, since most of the device is simulated with the classical MC technique. In this regard, a recent work developed at our group is also able to provide larger integration boxes for solving the Liouville equation [Garcia 1998]. The QW extends asymmetrically at both sides of the double barrier because the emitter region of the QW has to be large enough to define the initial Gaussian wavepacket in a flat potential region.

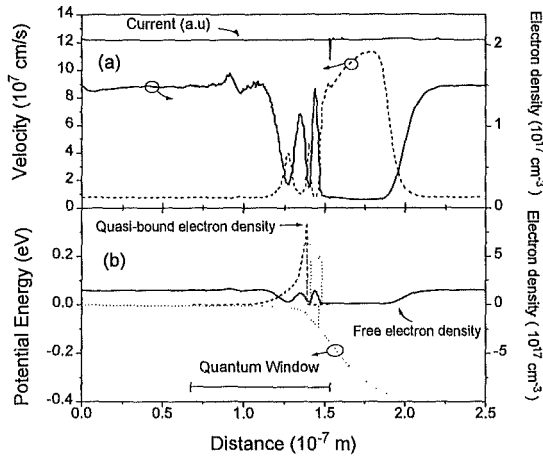


Figure 3.5: Self-consistent results of 3.0/5.1/3.0 nm double barrier GaAs/AlGaAs RTD at 77 K with an impurity density of $5 \cdot 10^{18}$ cm $^{-3}$ at a resonant bias of 0.39 eV: (a) Electron density (solid line) and average velocity (dashed line). The upper horizontal solid line represents the current density (in arbitrary units) computed as the product of the average charge density per average velocity. (b) Self-consistent potential profile (dotted line) and electron density: due to free electrons (solid line) and to quasi-bound electrons (dashed line).

In figure 3.5 we show self-consistent results obtained at a particular bias point of 0.39 V, corresponding to a position close to the peak of the I-V curve. The results shown obtained by averaging instantaneous results over 1000 iterations after reaching the steady-state particle distribution (2000 iterations are usually required to reach it; the time step between iterations being $\Delta T=5$ fs). In fig. 3.5(a) we represent (solid line) the electron density, which exhibits pre-barrier oscillations and an accumulation in the well. No technical spurious discontinuities are detected at the boundaries of the QW, this being an indication of the smoothness of our classical-to-quantum matching model (in this case we have used model A). In dashed line we represent the average velocity, which is inversely proportional to the charge density, since their product must be position-independent to assure current uniformity along the device (see fig 3.5). In this regard, the behavior in the collector depletion region is illustrative. It can be observed that the electrons travel faster in the depletion region because of the high electric field and, as a consequence, the electron density decreases in adequate proportion to maintain an uniform current. As reported by other authors [Frensley 1990], depletion is also obtained in the emitter pre-barrier region as a consequence of the fact that electrons travel ballistically inside the QW. As we have said, the fact that no scattering is considered inside the QW has important consequences on the self-consistent results. To obtain an accumulation layer in the emitter region adjacent to the first barrier, the charge associated to quasi-bound states should be taken into

account. However, since scattering in the QW is not considered yet, these states are unreachable from Bohm trajectories. To avoid this unphysical result, a semi-classical Thomas-Fermi approximation [Fiig 1991] has been used to compute this additional charge [see fig. 3.5(b)]. This electron charge is added to the MC charge obtained from expression (3.5) before solving the Poisson's equation.

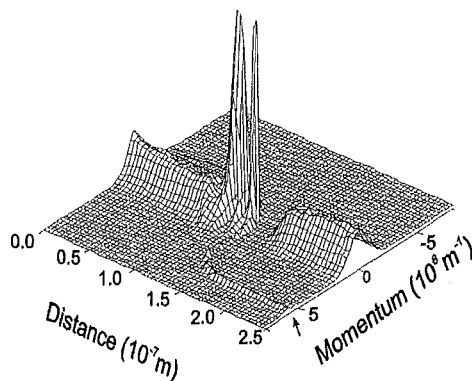


Fig 3.6: Phase space distribution function along the device of Fig. 3.5. Notice the tunneling ridge (indicated by an arrow), which is originated in the QW by resonant Bohm trajectories and which becomes progressively thermalized in the collector by scattering mechanisms.

As we have previously discussed, in addition to the results such as those obtained for charge and current densities, the use of causal trajectories allows one to obtain more information related to the hidden variables. In particular, the use of Bohm trajectories directly leads to the existence of the classical-like phase-space distribution. In fig. 3.6 we have represented the particle phase-space distribution at the resonance voltage, obtained from expression (3.6) averaging over the last 1000 iterations. This distribution is qualitatively quite similar to the Wigner Distribution Function solution of the Liouville equation, but it must be stressed that, contrarily to Wigner function, our phase space distribution is positive by construction. On the other hand, we notice the presence of a tunneling ridge in the collector which was also reported within the Wigner function framework [Frensley 1990]. Electrons in the collector depletion region mainly come from Bohm trajectories associated with resonant wavepackets. Since these resonant trajectories behave ballistically, a number of electrons with large momentum appear in the collector. The presence of these resonant hot-electrons, which are thermalized along the collector, is responsible for the net current density at the right boundary of the QW. Very few electrons, with high velocities, are responsible for the current in the collector. On the contrary, the whole wavevector distribution is shifted towards positive momenta in the emitter, so as to give an uniform current density.

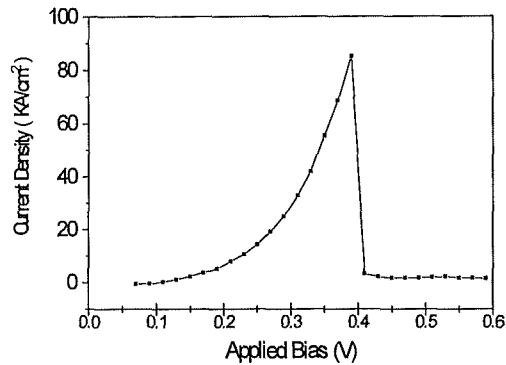


Fig. 3.7: I-V curve of the double barrier GaAs/AlGaAs RTD described in fig. 3.5.

Finally, in fig. 3.7 we present the self-consistently simulated current-voltage characteristic of the RTD described above. At the initial bias of 0.07 V, an arbitrary particle distribution is defined, and it evolves during 3000 iterations until the steady-state is reached (lower voltages are not considered since no electron transport from collector to emitter is implemented). In order to reduce the transient time required to reach the steady-state, the particle distribution obtained for one bias point is used as the seed for the next one. The current density is determined by averaging expression (3.8) over the last 100 iterations. A sharp resonant peak is obtained in the I-V curve at an applied bias of 0.39 Volts. The whole I-V curve is very similar to that obtained from a fully coherent treatment based on the solution of the stationary effective-mass Schrödinger equation. This is an expected result since we are not considering scattering in the QW.

3.4.- Connection of our approach with the Liouville equation

At this point, it can be interesting to establish the relation of our approach with the those based on the solution of the Liouville equation (the density matrix and the Wigner function). With this aim in mind, let us consider a steady state situation for our device. In this particular case, the classical distribution function, $f(\mathbf{k})$ at the boundaries of the QW is time independent. This means that a constant flux of electrons arrives at the boundaries of the QW. This constant flux can be modelled by a SISOW inside the QW. If we suppose that no scattering is present in the QW, the classical distribution function, $f(\mathbf{k})$ is also valid to define the occupation probability of each